Zebrafish behavioral, physiological, and neural response to anesthetic compounds

A THESIS PRESENTED
BY
HANA ROSTAMI

PRESENTED TO
THE FACULTY OF THE COMMITTEE ON DEGREES IN NEUROSCIENCE
IN PARTIAL FULFILLMENT OF THE REQUIREMENTS
FOR THE DEGREE OF
BACHELOR OF ARTS

HARVARD COLLEGE
CAMBRIDGE, MASSACHUSETTS
MARCH 12, 2026

The Harvard College Honor Code

Members of the Harvard College community commit themselves to producing academic work of integrity — that is, work that adheres to the scholarly and intellectual standards of accurate attribution of sources, appropriate collection and use of data, and transparent acknowledgement of the contribution of others to their ideas, discoveries, interpretations, and conclusions. Cheating on exams or problem sets, plagiarizing or misrepresenting the ideas or language of someone else as one's own, falsifying data, or any other instance of academic dishonesty violates the standards of our community, as well as the standards of the wider world of learning and affairs.

The Neuroscience Concentration AI Policy

Completing a thesis develops valuable skills in analytical thinking and scientific writing. **Students are strictly forbidden from including AI-generated content in any part of their thesis manuscript, including preliminary drafts.** Incorporating AI-produced text into your thesis constitutes an Honor Code violation at Harvard College and will be considered academic misconduct.

Certain applications of generative AI tools are acceptable during other research phases. For example, these tools may be valuable for broadening or deepening your knowledge of specific concepts, understanding methodologies, or troubleshooting analyses. However, exercise caution when using these resources: current AI models regularly produce inaccurate information. This is especially true for scientific research, as journals are often paywalled and thus under-represented in training data.

You bear full responsibility for the accuracy of all assertions in your thesis, making it essential to rigorously verify any AI contributions. You should be prepared to answer questions about any part of your thesis during the oral conference.

If you are unsure as to whether a particular use is allowed, contact your concentration advisor promptly.

By signing below, I confirm that I have adhered fully to all components of the Honor Code and AI Policy in the production of this thesis.

Digital Signature:

تقدیم به مامان و بابا. من همه چیز را مدیون زحمات شما هستم.

Acknowledgments

I would like to thank my Principal Investigator, Florian Engert, for his continuous support. From generating unparalleled excitement for systems neuroscience in MCB 105 to supporting this project over the past two years, he has been an invaluable source of guidance and encouragement.

I would also like to thank my research mentor and supervisor, Nikolai Hörmann. Thank you for giving me the space to explore, learn, and make mistakes, while being incredibly generous with your time and patient in answering every question I had throughout this process. Working with you has been one of the most rewarding parts of completing this thesis.

I would also like to thank all of the members of the Engert Lab. I am grateful for the intellectually stimulating environment that this lab has provided, allowing me to grow as a student and researcher. Being part of this lab has shown me how enjoyable and fulfilling research can be.

To my parents, Nafiseh and Reza: your unwavering support throughout my life and during this thesis is beyond what words can describe. Maman, thank you for being my best friend in life. You always inspire me to push harder and keep moving forward. I owe the

person I have become to you. Baba, you are the reason I fell in love with studying neuroscience, a passion that has culminated in this thesis. You taught me to ask questions with curiosity and to seek answers relentlessly. I strive to be as driven and dedicated as you are. Tara, your patience and mindset inspire me every day. I am so lucky to have you as my sister.

To Sima, Hossein, and Liana: you are the best second family I could have asked for. Thank you for your endless support every step of the way—not just during the completion of this thesis, but throughout every new challenge I have undertaken. You have been my biggest cheerleaders at every milestone, and I would not be here without your unconditional support.

To my wonderful friends: thank you for listening to me talk about my fish for hours on end and for encouraging me as I completed this thesis and made endless visits to the BioLabs. You have made Cambridge feel like a home away from home over the past four years. Each and every one of you has touched and changed my life in a special and lasting way. I am deeply grateful for your friendships and hope to cherish them for years to come.

Contributions

All experiments and analysis performed as part of this thesis were done by Hana Rostami, with the exception of the whole-brain light-sheet imaging which was performed by Marc Duque and the light-sheet imaging atlas alignment which was performed by Nikolai Hörmann. Kristian Herrera created and developed the set-up and code used for heart-rate imaging tracking. Zebrafish husbandry was performed by Hana Rostami and Nikolai Hörmann, and the preparation of zebrafish for experiments was done by Hana Rostami. Nikolai Hörmann helped discuss and develop the experimental and analytical methodology employed in this thesis. Nikolai Hörmann and Marc Duque provided guidance with data analysis. Marc Duque developed the preliminary code which was adopted for some of the initial light-sheet pre-processing. Roy Harpaz helped discuss the free-swimming social behavior methodology and metrics.

Thesis advisor: Professor Florian Engert Hana Rostami

Zebrafish behavioral, physiological, and neural response to anesthetic compounds

Abstract

Anesthetics have revolutionized modern medicine by enabling the safe and painless performance of invasive medical procedures. However, even widely used compounds can have life-threatening side effects. It is therefore essential to understand the mechanisms of anesthesia and to develop new anesthetic compounds. Although several molecular pathways are known, the system-wide dynamics of anesthesia are not fully understood. Larval zebrafish (Danio rerio) offer a unique opportunity as a vertebrate model to investigate anesthetic mechanisms due to their conserved physiology, measurable behavior, and optical transparency. This thesis investigates the behavioral, physiological, and neural responses of zebrafish larvae to established anesthetic compounds (ketamine and propofol) and presents the first zebrafish quantification of ketofol (a mixture of ketamine and propofol) and a newly developed compound, WB3. Cardiovascular measurements revealed that ketamine has relatively modest effects on heart rate, followed by ketofol, propofol, and WB3, the latter causing the most acute decline in cardiac activity. Free-swimming behavioral assays showed that higher concentrations of propofol and WB3 significantly perturb locomotor behavior, whereas ketamine-treated larvae displayed partial recovery. WB3 was associated with slow and ineffective anesthesia recovery and increased mortality at higher doses, suggesting limited anesthetic potential for the compound. Light-sheet imaging analyses identified strong locus coeruleus suppression to be associated with deep anesthesia and lack of recovery. We also identified sensory and motor nuclei in which increased activity is associated with locomotor restoration after anesthesia. The findings of this thesis establish a framework for comparing anesthetic efficacy and deciphering the mechanisms of anesthesia in larval zebrafish.

Contents

1

Introduction

The development of anesthesia has been a pivotal milestone in the history of humankind. The advent of modern general anesthesia was a notable step in enabling physicians to perform invasive surgical procedures and minimize pain under adverse conditions. The first modern instance of the use of general anesthesia in humans dates to 1846, when the first surgical procedure with ether gas as general anesthesia was performed in Massachusetts

General Hospital (Robinson and Toledo, 2012). During the 1840s, a variety of gases including diethyl ether, nitrous oxide, and chloroform were used as general anesthetics (Robinson and Toledo, 2012). Nevertheless, despite the significance of general anesthesia in advancing medicine, few major breakthroughs have occurred regarding the discovery and development of new anesthetic compounds. Furthermore, the transition of many procedures from a hospital-only setting to outpatient clinics where patients tend to be older and more vulnerable represents a shift in medical practice that highlights the need for new and better compounds (Chitilian et al., 2013).

More specifically, rapid onset of action and recovery, and minimal side effects such as nausea, vomiting, psychosis, and pain are characteristics that would improve anesthetic use (Chitilian et al., 2013).

In addition to having anesthetic properties, an ideal anesthetic compound should preserve vital physiological functions and not cause acute changes in breathing and cardiac function. Because many anesthetics depress the Central Nervous System (CNS), the brainstem circuits responsible for breathing and cardiac activity can also be disrupted. Suppression of heart activity and respiration during anesthesia can have drastic consequences such as hypoxia and tissue death, and in severe cases, death. Thus, it is imperative to study the effect of anesthetic compounds on physiological function. Maintaining stable heart and respiratory function while achieving adequate sedation is the desired outcome.

Compounds that bring about general anesthesia act primarily by modulating the CNS to suppress neuronal activity and induce a reversible state of unconsciousness and analgesia, which can be achieved through different chemical and biological pathways. These effects are generally achieved by enhancing inhibitory transmission (e.g., via $GABA_A$ receptor potentiation) or through silencing excitatory pathways (e.g., NMDA receptor antagonism) (Son, 2010). μ-opioid receptors can also be modulated to produce an analgesic effect without necessarily bringing about full unconsciousness (García-Domínguez, 2025).

1.1 Neural Circuitry of General Anesthesia

Although anesthetic compounds have been used extensively for decades, their specific mechanism in the brain remain unclear. Most of what is known about anesthetic activity is limited to the receptor and neuronal level, but the interconnectedness of the brain means that there are further large-scale effects that are poorly understood (Shin et al., 2022).

Anesthesia can generally be defined as a loss of consciousness and a state where the organism or individual is incapable of feeling pain. Generally, the activity in the brain is reduced during anesthesia. Stimulating the thalamus and locus coeruleus has been shown to counteract the effects of anesthesia, reducing time required for emergence and increasing arousal in mice (Ao et al., 2021). Similarly, in humans, thalamic lesions show that the thalamus is crucial for consciousness (Cacciatore et al., 2025). Moreover, Reed and Plourde

(2015) showed that anesthesia is associated with an attenuation of high-frequency electroencephalogram (EEG) markers in the thalamus, localizing to some extent the areas affected during general anesthesia.

1.2 Anesthetic Compounds Under Investigation

1.2.1 Propofol

Propofol is a fast-acting intravenous anesthetic compound. It is widely used because of its fast metabolism in the liver. It reduces blood flow to the brain and subsequently, cerebral metabolism and intracranial pressure. It results in less nausea and vomiting in patients compared to other compounds, making it an appropriate compound for widespread clinical use (Lundström et al., 2005). On a molecular level, it is believed to target $GABA_A$ receptors to induce anesthesia (KE Brown et al., 2013). It induces a large Cl^- current, bringing about hyperpolarization (Bademosi et al., 2018). Propofol does not directly target nociceptive pathways and does not have an analgesic effect; it induces a state of unconsciousness so that the patient does not feel painful stimuli (Sahinovic et al., 2018). The reduced vascular resistance from propofol is the effect of sympathetic nervous system depression and not a direct consequence of propofol activity (Sahinovic et al., 2018).

Propofol-induced anesthesia has been associated with an increase in low-frequency (<1 Hz) signals and reduction of alpha (8–13 Hz) oscillations. Conversely, emergence from

propofol-induced anesthesia has been shown to closely correlate with an increase in alpha amplitudes at low-frequency oscillations (Purdon et al., 2013). On a system-wide level, propofol impairs feedback from parietal signaling while forward connections are preserved. In humans, propofol affects the Default Mode Network (DMN) involved in cognitive activities. It is hypothesized that part of the anesthetic effects of propofol are brought about by the inhibition of reticular arousal mechanisms in the brainstem (Guldenmund et al., 2017).

In zebrafish, Du et al. (2025) found that propofol inhibits norepinephrine release from individual locus coeruleus-norepinephrine (LC-NE) neurons, highlighting the role of the locus coeruleus (LC) in general anesthesia. LC has previously been established to be closely involved in modulating cognition and arousal, highlighting the potential role that this region would play in the mechanism of general anesthesia (Sara and Bouret, 2012).

However, despite its widespread use, propofol carries the risk of cardio-respiratory depression. It is particularly risky in patients with epilepsy, where seizures have been reported in the past (Lundström et al., 2005). This can pose a significant risk for vulnerable patient populations and widespread propofol use.

1.2.2 Ketamine

Ketamine is another commonly used anesthetic. Ketamine acts on nicotinic, muscarinic, opioid, and NMDA receptors. Chemically, ketamine is a mixture of two isomers, R- and

S-ketamine. The former is a strong NMDA pore blocker, although the majority of medically available ketamine is a mix of both isomers given the difficulty of separating the two stereoisomers (Hashimoto, 2019). Ketamine prevents sensitization in the superficial dorsal horn by blocking sodium and potassium channels. Dorsal horn neurons in the laminae I–III of the spinal cord play a vital role in pain sensitization and transmission, and they are thus the primary pharmacological target of spinal anesthetic drugs (Schnoebel et al., 2005).

On a molecular level, at lower doses, ketamine preferentially binds to NMDA receptors on GABAergic inhibitory interneurons, resulting in the diffusion of excitatory activity throughout the cortex (Seamans, 2008). When administered in higher doses, ketamine blocks NMDA receptors present on excitatory pyramidal neurons that exist throughout the brain and the CNS (EN Brown et al., 2018). Moreover, ketamine also disrupts the frontal to parietal lobe connectivity and interferes with frontal lobe connectivity to other DMN locations. Cortico-cortical interactions are also reduced after ketamine administration, while thalamocortical connectivity is increased (Höflich et al., 2021).

Previous studies on the effects of ketamine on the zebrafish brain have shown suppressed neural activity in early visual areas and hindbrain motor regions, which is consistent with ketamine's inhibitory effects on spontaneous movement and response to sensory stimuli (Duque et al., 2025).

The mechanism of ketamine activity is different from most other anesthetic compounds

because its depressive effects on the cardiac and respiratory systems are much less pronounced (Mion and Villevieille, 2013). The hemodynamic effects of ketamine are mostly indirect and are a consequence of sympathetic stimulation, resulting in increased heart rate. However, the direct effects of ketamine on inotropy, the contractile strength of heart muscles, are negative (Kongsayreepong et al., 1993). Given its cardiac profile, ketamine was used in battlefield surgical procedures such as the Vietnam War and is used for those at the risk of hypotension (Denomme, 2018).

Ketamine brings about a notably different form of anesthesia commonly referred to as dissociative anesthesia, where sensory inputs might reach the cortex but are not consciously perceived and processed (Mion and Villevieille, 2013). A major concern with the use of ketamine as an anesthetic and analgesic is its potential to induce cognitive disturbances and psychotic symptoms (Davis et al., 2021). Although it is a fast-acting compound, ketamine is not widely used for general anesthesia in humans due to the possibility of hyperexcitation in patients after recovery (Kohtala, 2021).

1.2.3 WB3

Although propofol is widely used in clinical settings and ketamine can be a potent tool for emergency anesthesia administration, both compounds have significant limitations. Propofol causes significant cardiac suppression while ketamine is associated with psychosis. The drawbacks associated with commonly used anesthetics highlight the need to develop

and evaluate new anesthetic compounds with enhanced characteristics.

A recently developed compound under investigation is WB3. WB3 is an SNC80 derivative. SNC80, originally intended to be a nonaddictive pain control agent, is a synthetic compound known for its high selectivity as an agonist of the δ-opioid receptor (Sperry et al., 2024). SNC80 was found to have a reversible but fast effect on biochemical activity, inducing anesthesia and analgesia, while preserving tissue viability (Sperry et al., 2024). Although useful for pain management and the targeting of mood disorders, clinical applications of SNC80 have been limited due to adverse side effects, namely convulsions at higher doses (Danielsson et al., 2006). Efforts have been made to isolate the antidepressant and analgesic effects of SNC80 from its convulsive effects. Jutkiewicz et al. (2005) found that slowing the rate of administration could preserve the antidepressant effects without causing convulsions. Such findings increase the potential for the use of SNC80 and its analogs for their other pharmacological properties.

Metcalf et al. (2012) investigated the antinociceptive effects of various SNC80 doses in wildtype and δ-KO mice to test SNC80's potential as a δ-opioid receptor agonist. δ-KO mice lack the gene encoding the δ-opioid receptor, allowing for the analgesic properties of SNC80 to be studied. Metcalf et al. (2012) found that δ-KO mice exhibited lower antinociceptive responses when administered SNC80, but the effects were nonetheless present. This raises the question of whether modifying SNC80 to have a lower affinity for certain

receptor types can preserve its analgesic properties while reducing the risk of convulsions and dependence.

WB3 is structurally modified to have lower affinity for the δ-opioid receptor, but can still induce an anesthetic state. More specifically, WB3 lacks the distal basic nitrogen (N-ally group) that SNC80 has, which has been hypothesized to be a critical δ-opioid receptor pharmacophore. Chemically, at physiological pH, this nitrogen carries a positive charge which allows it to form a salt bridge with a conserved aspartate residue in the binding pocket. Loss of this nitrogen therefore would reduce binding affinity. Experimental results in tadpoles have shown that WB3 has less δ-opioid receptor activity than SNC80 by a magnitude of almost 1,000 (Sperry et al., 2024). Figure 1.1 by Sperry et al. (2024) shows the molecular structures of SNC80 and WB3; the latter lacks the N-allyl piperazine moiety.

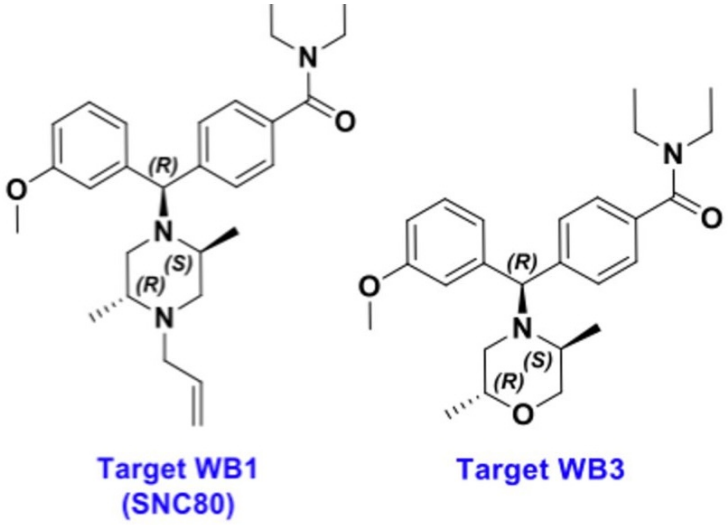

Figure 1.1: An overview of the structure of WB3 vs SNC80, adapted from Sperry et al. (2024)

1.2.4 Ketofol

Recent anesthesia research has explored the potential of using ketofol, a combination of both ketamine and propofol (Zaki et al., 2022). This is driven by the idea that using both compounds in conjunction could mitigate the adverse side effects associated with the high-dose single-compound administration of each anesthetic. Nevertheless, to our knowledge, other than studies in clinical settings, no behavioral or physiological quantification of ketofol response has been done in a controlled laboratory setting with model organisms.

1.3 Zebrafish as a Model Organism

Zebrafish, formally known as *Danio rerio*, can be used as a model to study the effects of novel anesthetic compounds. Zebrafish are vertebrates and are similar to humans in many aspects. Approximately 70% of human genes have one or more zebrafish orthologs. 47% of the orthologous genes have a one-to-one human-to-zebrafish mapping (Howe et al., 2013). Moreover, the number of protein-coding genes among zebrafish and mammals, including humans, is similar (Howe et al., 2013). Specifically, ion channel structure, neurotransmitters, and receptors share notable similarities in humans and zebrafish (Renier et al., 2007). These proteins are known to be involved in the organism's response to and recovery from anesthetic compounds (Forman and Miller, 2016). Notably, zebrafish express $GABA_A$ receptor subunits, NMDA receptor subunits, and opioid receptors, all of which are highly

conserved in mammals and are the primary targets of propofol, ketamine, and WB3, respectively (Forman and Miller, 2016; Howe et al., 2013).

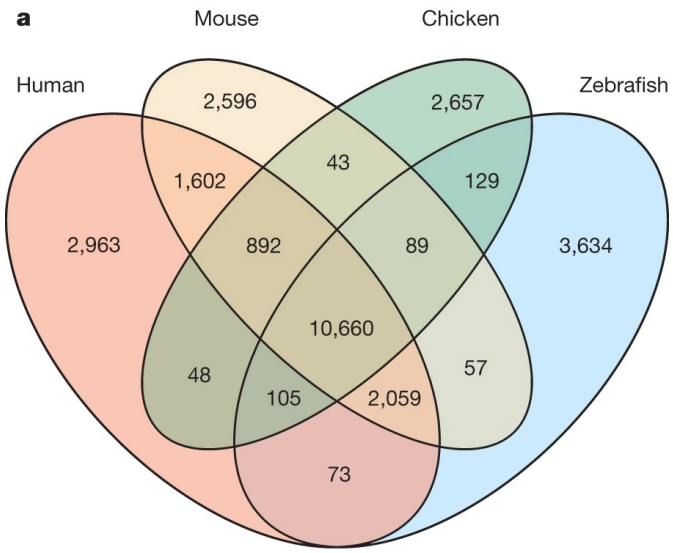

Figure 1.2: The number of orthologue genes shared between zebrafish, chicken, mouse, and human; adapted from Howe et al. (2013)

Moreover, a study of the endogenous opioid system in zebrafish revealed that this system is not significantly physiologically or structurally different from the mammalian system (De Velasco et al., 2009), underscoring the value of zebrafish as a model organism for investigating signaling pathways underlying pain management and anesthesia.

Furthermore, zebrafish larvae can breathe as oxygen diffuses through their skin (Kämmer et al., 2024), which allows anesthetics to be administered more easily by exposing the larvae to the treated solution. In addition, homozygous *nacre* mutant zebrafish lack melanophores and are optically transparent (Lister et al., 1999), allowing for heart and

brain imaging. Whole-brain imaging with transgenic zebrafish expressing calcium reporters can show levels of activity in most neurons of the brain (Ahrens et al., 2013). Ca^{2+} is used as a proxy for neuronal activity. GCaMP7 is one of the genetically encoded calcium indicators used to measure neuronal activity, increasing in fluorescence as Ca^{2+} levels rise (Dana et al., 2019). At 7 days post fertilization (dpf), zebrafish larvae are ~5 mm in length (O'Neale et al., 2014), facilitating embedding and imaging. Thus, given their transparency, zebrafish are unique as a model organism for studying the neural and physiological effects of compounds in vivo, especially at the whole-brain level.

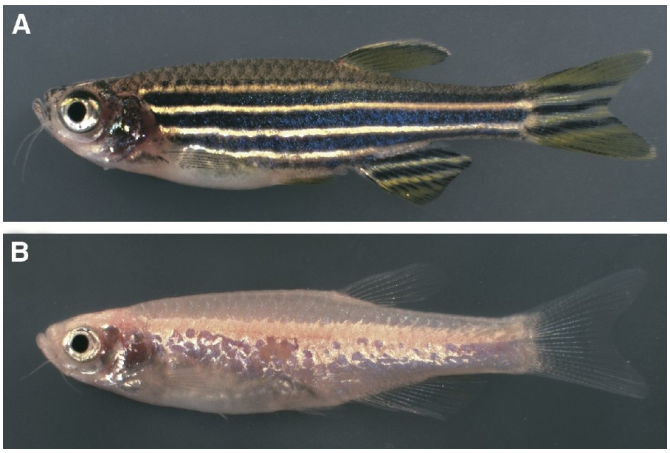

Figure 1.3: Image of wildtype (A) and homozygous *nacre* (B) zebrafish; adapted from Engeszer et al. (2004)

1.4 Zebrafish Behavior

Zebrafish swimming behavior is highly reliable and reproducible across different individuals. Zebrafish swimming is characterized by saccade-like tail bouts that propel the fish

forward and continuous gliding at a low speed (Mwaffo et al., 2017). The simple movement patterns of zebrafish larvae enable us to study motor control (Palmér et al., 2017) in the context of anesthesia.

One particularly useful behavioral assay to understand consciousness is the optomotor response (OMR), in which zebrafish instinctively swim in the direction of moving visual stimuli. This reflexive behavior is present in different species and helps the animal stabilize itself with respect to the direction of the movement of the visual field (Tanaka et al., 2023).

OMR requires intact sensory-motor integration, and its attenuation under anesthesia and exposure to anesthetic compounds provides a useful metric to assess CNS depression. Therefore, we can measure changes in optomotor behavior to assess the effects of anesthetic compounds. OMR depends on visual processing, sensorimotor integration, and coordinated motor output, all of which can provide a quantifiable readout of the nervous system's response to anesthesia. The re-emergence of robust sensorimotor integration can serve as a proxy of the recovery of consciousness.

1.5 Research Question

This thesis focuses on studying the anesthetic properties and mechanism of action of propofol, ketamine, WB3, and ketofol. More specifically, we aimed to investigate brain-wide responses and recovery while monitoring heart function and behavior. To accomplish

these aims, we 1) performed free-swimming locomotor assays to characterize zebrafish locomotor and optomotor responses to anesthetic compounds; 2) used free-swimming assays to quantify changes in zebrafish inter-individual distance and speed following recovery from anesthesia; 3) performed heart rate assays to evaluate the effects of these compounds on cardiac activity and physiological stability; and 4) used whole-brain calcium imaging to identify the brain regions and neural circuits involved in anesthesia induction and recovery. These behavioral, physiological, and neural responses were quantified with automated analysis pipelines to visualize changes across experimental conditions and compare different compounds.

Research Question:

What are the zebrafish dose-dependent behavioral, physiological, and neuronal responses to commonly used and novel anesthetic compounds (ketamine, propofol, WB3, and ketofol)?

2

Materials and Methods

2.1 Breeding and Embryo Collection

All free-swimming and head-fixed experiments used zebrafish from the *Danio rerio* species. All of the fish used for the experiments were homozygous for the *nacre* mutant, lacking melanophores. This mutant was chosen to allow for recording the heart rate of the organism during the head-fixed experiments using infrared cameras. Breeding was per-

formed in compliance with the standard breeding procedures approved by the IACUC. 8–10 adult zebrafish were placed in overnight breeding tanks and the embryos were collected the following day. The embryos were raised until they were used for experiments at 6 to 8 dpf.

2.2 Experiments

2.2.1 Free-Swimming

Two sets of free-swimming experiments were conducted, with and without visual stimuli. The dishes were round to avoid Snell's window, a refraction phenomenon in which an underwater observer perceives the above-water environment via a circular viewing cone of approximately 96º. Figure 2.1 demonstrates how the visual field of a fish is distorted due to the refraction of light at the water surface boundary, causing external stimuli to appear circular. Using circular dishes with angled walls reduced the refraction effects and minimized visual distortions.

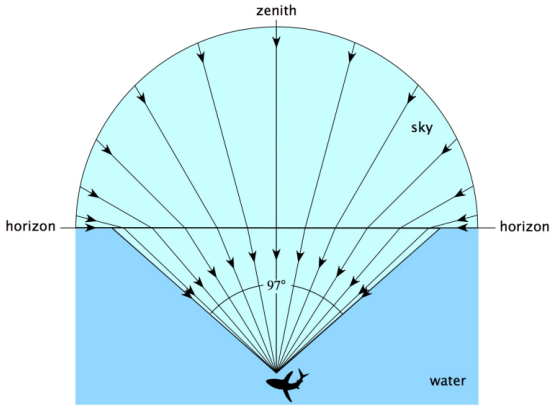

Figure 2.1: Schematic of Snell's window, adapted from Lynch (2015)

Moreover, clear petri dishes were not used for the experiments because the fish would be drawn to the corners of the dish upon seeing their own reflection, resulting in an inaccurate representation of their social behavior and increased tracking difficulty due to the sharp 90º angle at the edges of the petri dish.

2.2.1.1 Individual Free-Swimming

The first set of free-swimming experiments involved placing one 6–8 dpf fish in a 4.5 cm sandblasted dish. Each fish was tracked by a respective camera and shown a random assignment of one of three visual stimuli. The trials had either a stimulus with right-moving sine gratings relative to the fish, a stimulus with left-moving sine gratings relative to the fish, or no stimulus. This was intended to measure zebrafish visual responsiveness. The dishes were first filled with 5 mL of filtered fish water. A baseline swimming of fifteen minutes

was recorded to establish fish behavior in normal conditions. Then, the filtered fish water was removed and each fish was placed in a 5 mL solution of the respective anesthetic concentration. A treatment recording of 60 minutes was completed. After 60 minutes, the fish were washed out 3 times using filtered fish water and placed in 5 mL of filtered fish water. Recovery recording duration ranged from 120 minutes (ketamine) to 180 minutes (WB3) due to the different nature and recovery rates of each compound.

2.2.1.2 Social Free-Swimming

For the second set of free-swimming experiments, we wanted to examine the social behavior of zebrafish larvae post-exposure to the anesthetic compounds. 4–7 fish were placed in the same sandblasted dishes for the baseline, treatment, and recovery recordings. They were not shown a visual stimulus for this set of experiments since the primary aim was to examine spontaneous swimming behavior. The fish were similarly washed 3x after a treatment period that ranged from 60 minutes to 180 minutes, depending on the nature of the compound and the strength of the concentration being tested.

2.2.2 Head-Fixed

The homozygous *nacre* fish were head-embedded in 2% agarose made with filtered fish water. The tail of the fish were freed to study their movement and mimic a more natural physiological response. The head-embedded setup consisted of four infrared cameras each

simultaneously tracking four head-embedded fish at 200 frames per second. Projectors were used to project closed-loop grating visual stimuli from the bottom. A 4x objective was used to get a higher resolution of the fish for the heart rate tracking.

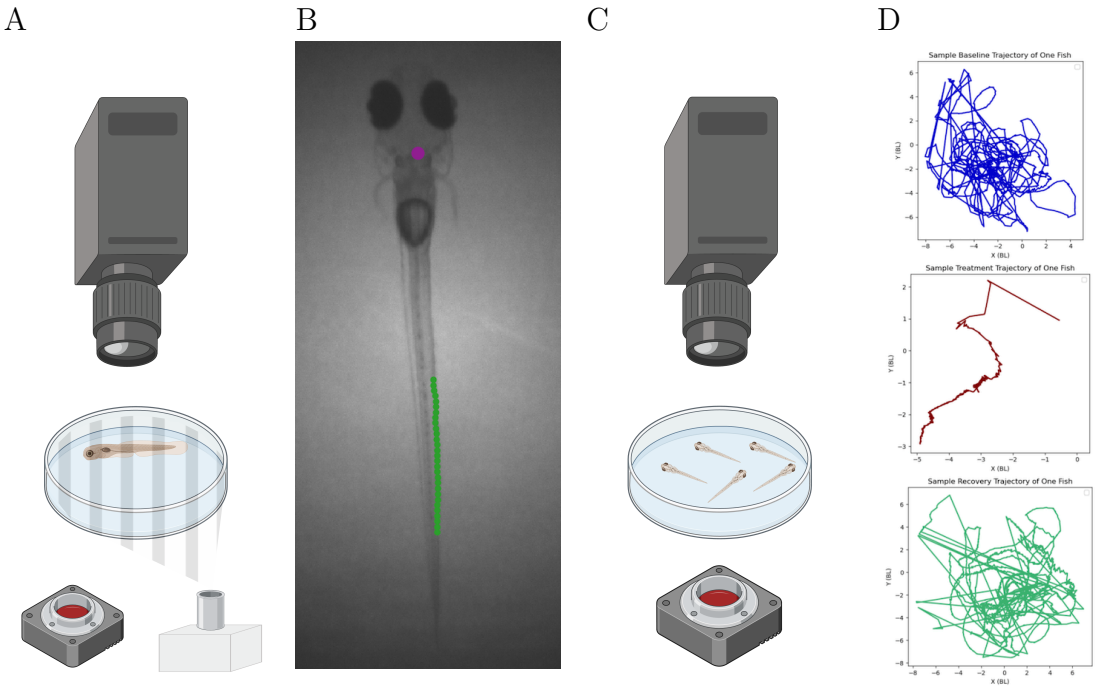

Figure 2.2: Behavioral assays and representative locomotor trajectories (A) Individual free-swimming set-up (B) Head-embedded tail-free fish (C) Free-swim setup (D) Example trajectories (top to bottom: baseline, treatment, recovery)

2.2.3 Light-sheet Imaging

Light-sheet fluorescence microscopy was used to assess brain-wide activity in larval zebrafish before, during, and after exposure to propofol. 7 dpf Tg(elav3:H2B-GCaMP7f) larvae were used for both sets of experiments and were immobilized by embedding in agarose to minimize motion artifacts and allow for accurate imaging. Propofol was perfused during *in vivo* imaging for more controlled solution delivery and washout. Whole-brain volumetric images were acquired by scanning z-planes across the plane.

2.2.4 Optomotor Response

To assess the fish optomotor response in free-swimming fish, trials were done under three stimulus conditions: right-moving sine gratings, left-moving sine gratings, and no visual stimulus. Optomotor response and sensorimotor integration would be required for the fish to have turning angles in the direction of the moving stimulus, thus serving as a behavioral metric for anesthesia recovery. Turn angles were calculated by subtracting the heading angle of the fish at the end of a recorded bout time stamp from the heading angle at the beginning of the recorded bout. This gave us a measure of the turn angle distribution of the fish to be examined for each stimulus and compound.

2.3 Compound Sources

Table 2.1 summarizes the compounds and concentrations that were tested for each experimental set-up. The solutions were all diluted with filtered fish water.

Compound	Source
Ketamine	Ketamine hydrochloride, from Patterson Veterinary, Cat#07-803-6637
Propofol	2, 6-Diisopropylphenol, %97 purity, from Sigma-Aldrich, Cat#D126608
WB3	Supplied by collaborators in the Wyss Institute

Table 2.1: Compounds used and their respective sources

Propofol is hydrophobic and lipophilic, requiring an organic solvent. Propofol was prepared in the laboratory by diluting 3.6 μL propofol in 1 mL of dimethyl sulfoxide (DMSO) to make a 20mM propofol stock solution. The resulting propofol solution was diluted with filtered fish water, as with other compounds, to reach the desired concentration.

2.4 Data and Analysis

2.4.1 Individual Free-swimming Analyses

The individual free-swimming setup simultaneously recorded and tracked the swimming fish. An algorithm developed and published by Bahl and Engert (2020) used background subtraction to detect the movement of the fish within the petri dish and record bout and stimulus information. The recordings were then analyzed in Python. To ensure the accu-

racy of the aggregate analysis for each concentration, individual fish bout rates were analyzed to determine if the fish was tracked or not. Fish that were not properly tracked were excluded from the final analysis.

2.4.2 Social Free-swimming Behavior Analyses

The social free-swimming experiment raw videos were pre-processed using Fiji ImageJ to perform a manual background subtraction with a rolling parameter of 5 pixels and disabled smoothing and background options. This was done for videos where initial tracking was not able to detect all fish. The videos were analyzed using *idtrackerai*, a deep-learning algorithm developed by Heras et al. (2019) for tracking the movement of freely moving animals. Figure 2.3a shows an example of fish tracked with *idtrackerai*. *idtrackerai* uses convolutional neural networks to identify and track individual fish in the recordings. The algorithm then generates training data from each video and creates individual identities for each tracked animal to ensure consistency across the recordings. During training, the program reports two quality-control metrics of positive pairs and negative pairs. The positive pairs metric quantifies the percentage of image pairs belonging to the same individual fish that were incorrectly classified as different identities, showing within-identity fragmentation. The negative pairs metric quantifies the percentage of image pairs belonging to different fish that were classified as the same fish. Because we could not establish pairing between individual fish from the baseline recording to the recovery recording, we did not use a paired

t-test. Instead, we used a Welch's t-test, which does not assume equal variances and is an independent two-sample t-test.

The results were analyzed in Python with custom code and using the `trajectorytools` package, also developed by the authors (Heras et al., 2019).

To ensure comparability between baseline and recovery social behavior, and that any observed differences could be attributed to altered movement patterns and potential social modulation rather than residual anesthetic effects on reduced locomotion, analyses were restricted to recovery frames that occurred after the mean movement speed had returned to 80% of the respective baseline speed. Figure 2.3b shows a schematic of the movement recovery timeline and how the active frames are detected once the speed is at 80% of the baseline threshold speed. Given the variability of baseline recordings and differences in movement patterns across fish from different batches of crosses, each recovery video was compared to the corresponding baseline video with the same group of fish.

To understand changes in the social behavior of zebrafish, we looked at inter-individual distance (IID) between the fish before and after anesthesia exposure.

For IID, in lieu of comparing the raw distance between individual fish during the baseline and recovery recordings, which are greatly influenced by speed and group density, we adopted a shuffled-baseline approach to isolate non-random changes that would be produced by the treatment. The shuffled IID distribution was calculated by computing a

probability density function (PDF) of the expected distance between fish as predicted by random chance, determined using the number of fish in the dish and the overall speed. The distances were reported in body lengths (BL), which were set to 100 pixels as a constant assumption for all recordings. We then calculated the ΔIID, defined as the difference between the observed IID and the shuffled distance. This metric shows whether the fish are closer or farther away than what we would expect to see under random motion. Figure 2.3c shows a schematic of the inter-individual distance PDF and the calculations.

2.4.3 Heart rate Analyses

For the head-embedded experiments, the heart rate was tracked using a Python algorithm developed by Kristian Herrera in the Engert laboratory. The results were then analyzed using custom code in Python. The system recorded the heartbeats using a background-subtraction approach. The focal position of interest was chosen before starting the experiment and set to the location with the greatest contrast in intensity as the heart pumped blood. We developed a peak-detection approach to detect the peaks within the recorded signal and extract the heartbeat frequency across each stage.

Figure 2.3d is a schematic representation of heart rate peak detection. To pre-process the data, a third-order Butterworth bandpass filter was used to remove high-frequency noise >8 Hz and low-frequency drift <0.5 Hz. Peak detection was then performed using the `find_peaks` function in the `scipy` package. The height threshold was set to the 80th

percentile of the signal amplitude to ensure the detection of true heart beats. Also, a minimum inter-peak distance of 0.2 seconds was determined. This corresponds to a maximum heart rate of ~300 beats per minute, which is consistent with the upper end of zebrafish heart rate reported by existing literature, ensuring that noise is not captured. Lastly, peak prominence was calculated for each trial as the product of a scaling factor of 0.7 and the robust standard deviation of the filtered signal. This ensures that the peaks stand out relative to local variability. These three parameters were optimized iteratively and by visual confirmation of recording intervals to verify that as many peaks as possible were detected without capturing noise.

A

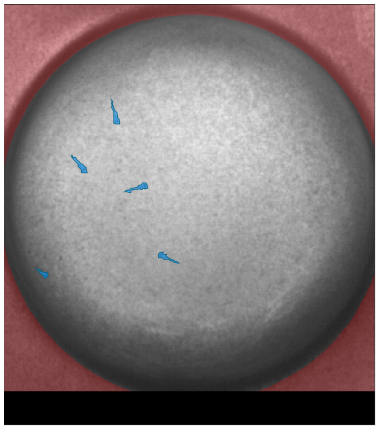

(a) Tracking with idtracker.ai.

B

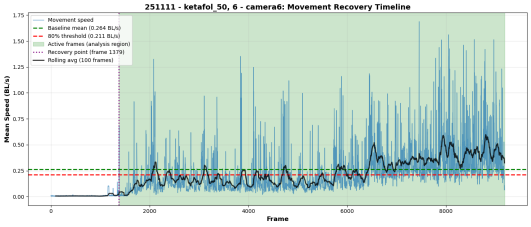

(b) Example of 80% movement recovery during anesthesia recovery.

C

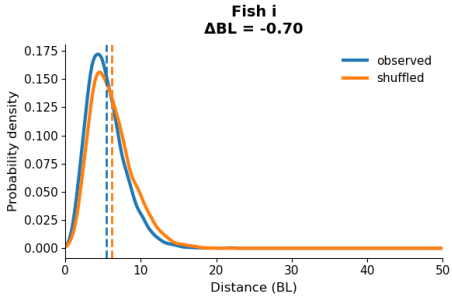

(c) Schematic of shuffled versus observed inter-individual fish distance.

D

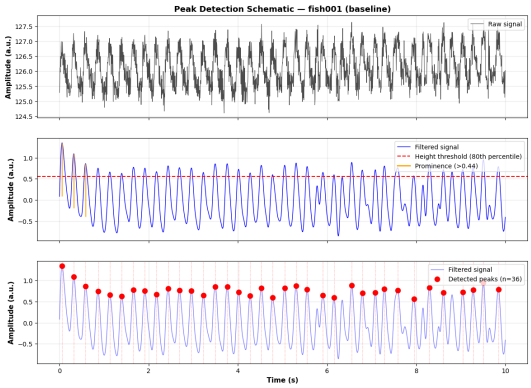

(d) Peak detection schematic.

Figure 2.3: Analysis methods overview (A) Tracking with *idtracker.ai* (B) Movement recovery quantification during recovery (C) Shuffled baseline comparison for inter-individual distance (D) Peak detection methodology

2.4.4 Whole-brain imaging analyses

To quantify the fluorescence changes in response to anesthetic administration, we computed $\Delta F/F_0$ for the period before and during the administration of the compound, and during baseline and after emergence. Every frame corresponds to one second. Baseline fluorescence (F_0) was defined as the average signal across the first 500 frames of the recording, after which the propofol was administered and washed out at frame 1500. To measure brain activity after propofol was administered, we defined the (F) as frames 750-1250 since it takes time for the propofol perfusion to be completed and replace the fish's chamber water with the propofol-treated water. $\Delta F/F_0$ was calculated as $(F - F_0)/(F_0)$. This is a normalized measure of change in fluorescence compared to the baseline window. Positive $\Delta F/F_0$ values indicated increased activity during treatment compared to baseline, and negative values reflect decreased activity.

3

Results

3.1 Free-swimming Locomotor Assays

We performed individual fish free swimming locomotor assays to measure anesthesia induction and recovery. These results show zebrafish locomotor and optomotor responses to anesthetics. Figure 3.1 shows the baseline normalized bout rate for all fish aggregated. The gaps between the phases in the plots are deliberate to highlight the discontinuous nature

of the recordings brought about by the need to replace the filtered fish water with the anesthetic solution and the 3x washout for treatment and recovery phases, respectively. While the swim bouts recorded during the treatment phase are partially due to the slower onset of anesthesia and any fish that may not have responded to the treatment, there is some noise associated with the recording. As seen in panel A, lower doses of ketamine have slower anesthesia onset, while higher doses display a faster loss of movement. By the end of the recovery period, all of the four tested concentrations have recovered to more than half of the normalized baseline bout rate. Panel B shows that fish treated with 15 μM propofol have higher normalized recovery bout rates compared to fish treated with 30 μM propofol throughout the recovery period. Panel C shows that the onset of anesthesia for WB3 100 μM is extremely rapid, such that there is almost no movement tracked after the fish are transferred to the anesthetic solution and the recording starts. Recovery, however, is much slower for both doses. Fish treated with 80 μM and 100 μM WB3 solutions are at a similar level of locomotor recovery after the conclusion of the two hour recovery period.

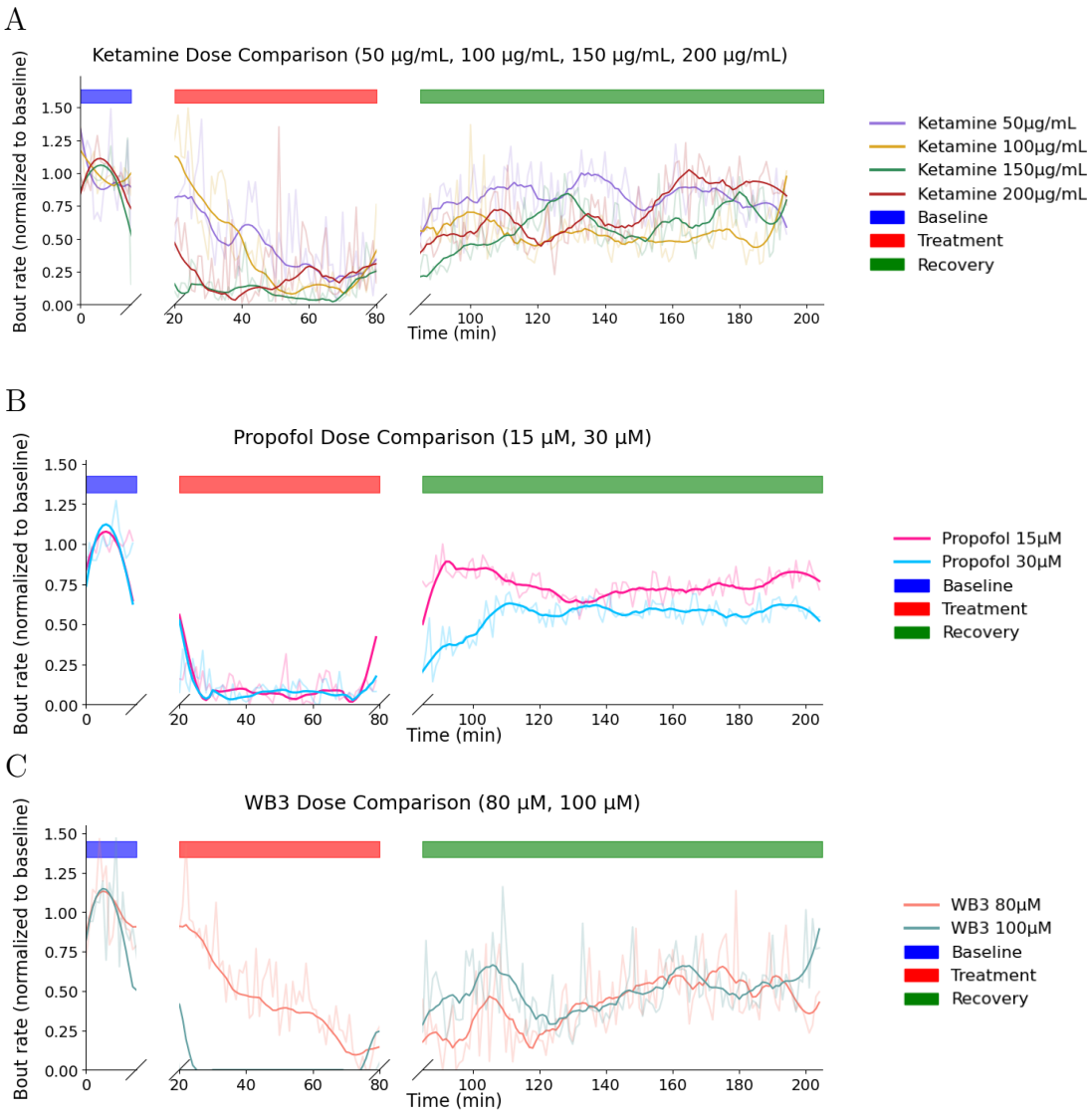

Figure 3.1: Baseline-normalized locomotor recovery for fish treated with different anesthetic concentrations (A) Ketamine (B) WB_3 (C) Propofol

3.1.1 Optomotor Response

Figure 3.2 shows the turn angle distributions for the individual free swimming zebrafish before and after anesthetic exposure when shown stimuli with right and left-moving sine gratings. Panels A and C show the recovery turning angle distributions for right and left-moving sine gratings for each concentration, respectively. The averaged baseline turn angle distribution across all experiments is shown with the dashed line. Panels B and D show the difference between the recovery and baseline turn angle distributions for every baseline-recovery pair of recordings for each fish, averaged across the tested concentration. Fish treated with ketamine have similar recovery and baseline turn angle distributions for both right and left-moving gratings. However, at 100 μg/mL ketamine, the fish did not turn as much compared to the other concentrations. Across all four concentrations of ketamine tested, turn angles corresponding to both right and left-moving grating stimuli show reduced directional sensitivity, with a higher density around a 0º turn angle.

For fish treated with propofol, recovery distributions are also similar to those of baseline. At the lower tested dose of 15 μM, recovery density distributions appear similar to the baseline curves. For the higher tested dose of 30 μM, the recovery turn angle distribution curves are more centered around 0º, indicating that the fish swim in straighter trajectories and make fewer turns.

At both WB3 concentrations tested (80 μg/mL and 100 μg/mL), turn angle distribu-

tions are similar between baseline and recovery. However, for both concentrations and both stimulus directions, the recovery distribution curves appear less uniformly distributed when compared to the globally averaged baseline, with the recovery curve at some points falling below the baseline curve. However, in panels C and D that show the Δ density, the values near 0º appear positive. This is explained by the fact that for the Δ density calculations, we used each fish's individual baseline and recovery, so a lower baseline for WB3 can explain this observation.

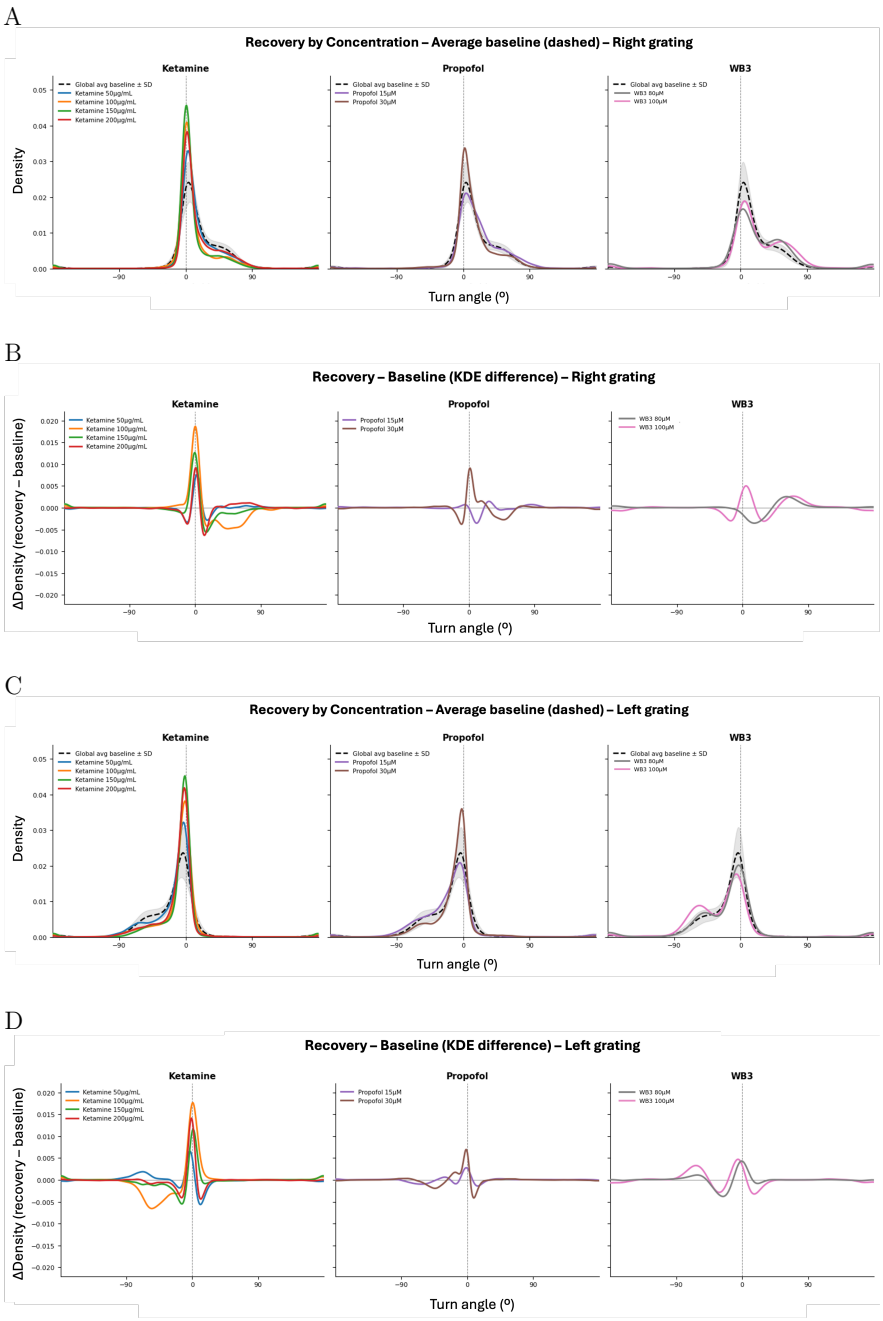

Figure 3.2: Turn angle dynamics density for right- and left-moving gratings pre and post exposure to different anesthetic concentrations (A) Turn angle distributions — right grating (B) Recovery minus baseline difference in turn angle — right grating (C) Turn angle distributions — left grating (D) Recovery minus baseline difference in turn angle — left grating

Figure 3.3 shows the difference between the observed and shuffled distances of fish for each concentration before and after anesthesia administration. The same batch of fish was used for each set of experiments to ensure consistency across the fish. The distance is measured in body lengths (BL), which were normalized to be 100 pixels. This is an average value and was set to facilitate the interpretation of results instead of reporting the observed distance in pixels; the comparisons are relative and the precise number assumed for the BL is arbitrary.

The results show that at ketamine 150 μg/mL, ketamine 200 μg/mL, and ketamine 250 μg/mL, there is a statistically significant decrease in the ΔIID. There is no directional difference associated with the strength of the administered ketamine dose and the recovery inter-individual distance dynamics. Moreover, fish treated with ketofol (ketamine 25 μg/mL and 3 μM propofol) and fish treated with 50 μM WB3 also show a decrease in the ΔIID after recovery. However, for propofol 30 μM, no significant reduction in this difference is observed.

Figure 3.4 shows the change in mean swimming speed, measured in BL per second (100 pixels per second) during baseline and recovery. There is no statistically significant change in the mean swimming speed except in fish treated with 200 μg/mL ketamine, although the variance is higher during recovery for fish across all anesthetics.

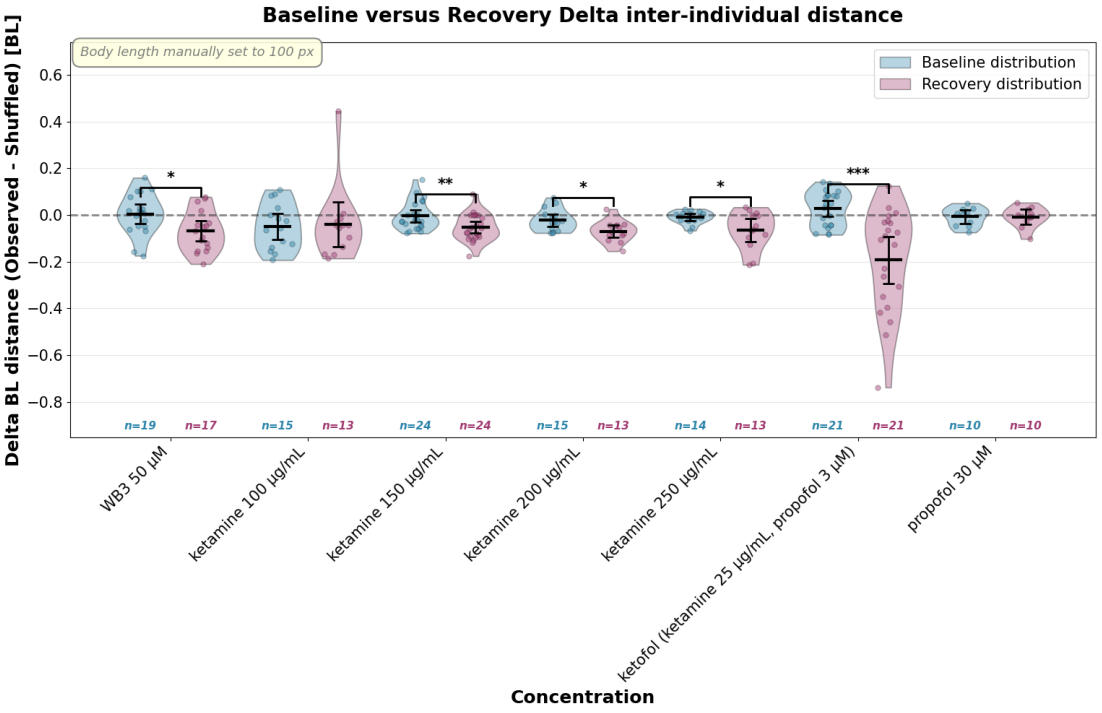

Figure 3.3: Change in inter-individual distance relative to a shuffled control (observed − shuffled), expressed in body lengths (BL). Bars show group means with error bars; points show individual fish.

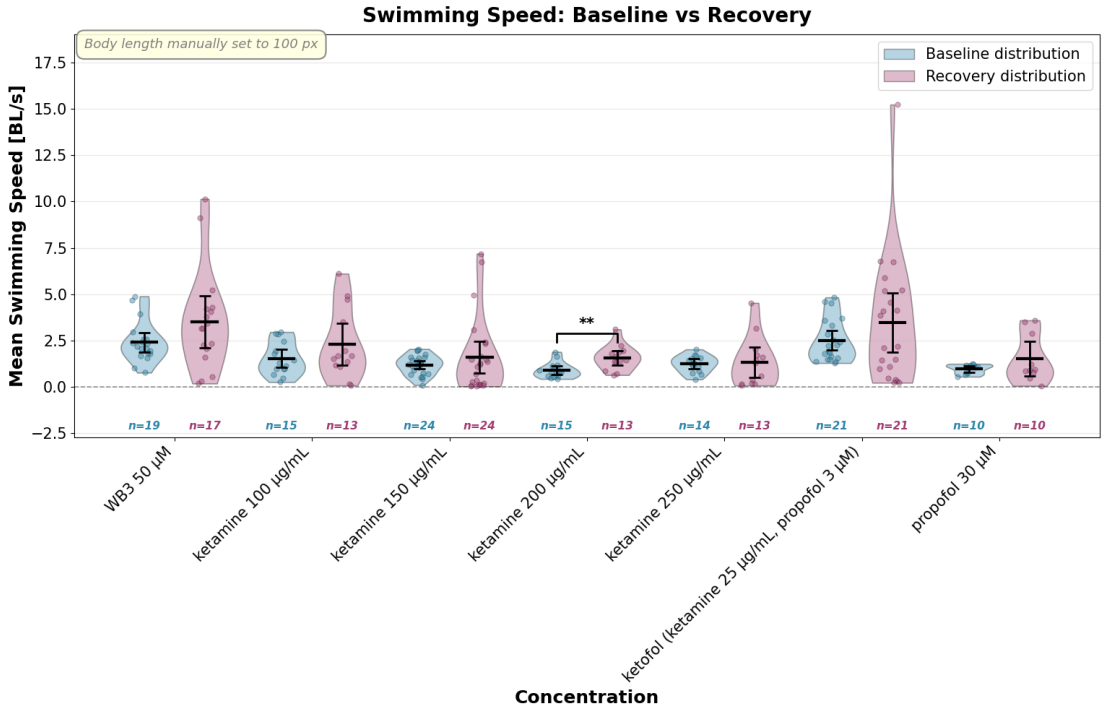

Figure 3.4: Mean swimming speed (BL/s) comparing baseline and recovery periods across concentrations. Bars show group means with error bars; points show individual fish.

3.3 Heart rate Recordings

To understand anesthetic effects on heart rate, we performed head-embedded experiments, recording the heart rate of zebrafish before, during, and after treatment. Zebrafish were embedded in agarose and their tails were freed to allow for spontaneous swim bouts. After a baseline recording, the filtered fish water in the petri dish was replaced with 5 mL of the anesthetic compound diluted with filtered fish water.

As seen in panel A of figure 3.5, ketamine exhibits the lowest variability in heart rate suppression, with all three tested doses producing little to change compared to baseline. At the intermediate dose of ketamine tested (200 μg/mL), there is a clear but transient dip in the heart rate at the beginning of recovery before convergence.

Panel B of figure 3.5 shows the heart rate changes in response to the five tested doses of propofol. At lower concentrations of 6, 10, and 15 μM, the effect on heart rate is modest and some recovery is observed. At higher doses of 30 μM and 50 μ0M, there is a sharp decline in the heart rate and no recovery is observed by the end of the recovery period.

Panel C of figure 3.5 shows the heart rate response to two doses of WB3. At 40 μM, the heart rate is relatively stable followed by a quick drop; 2 out of n = 4 fish were visibly dead at the end of the treatment period. At 80 μM, heart rate drops steadily throughout the treatment, and 3 out of n = 4 fish were visibly dead at the end of the treatment period. Thus, no recovery period is included for the WB3 heart rate recordings since the experi-

ments were stopped.

A

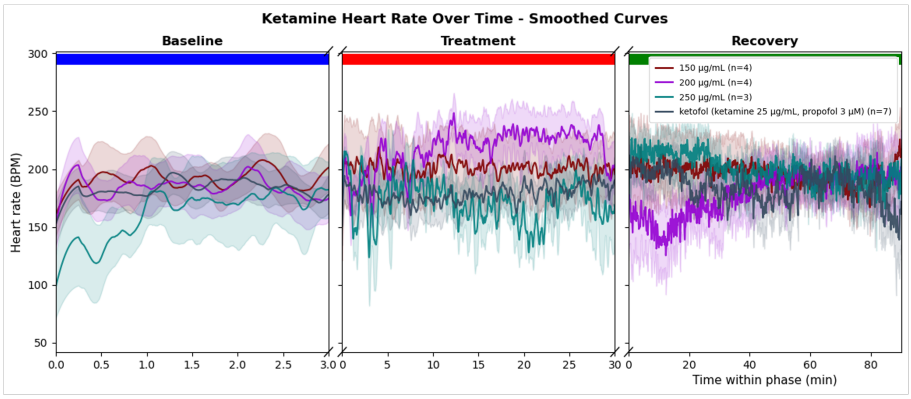

B

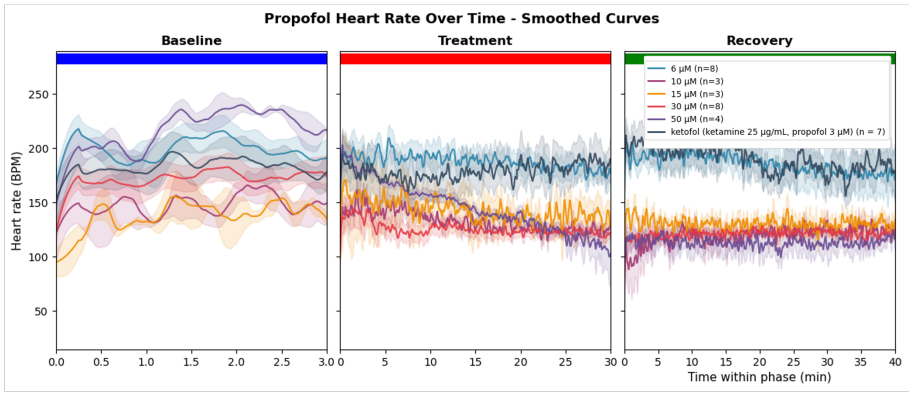

C

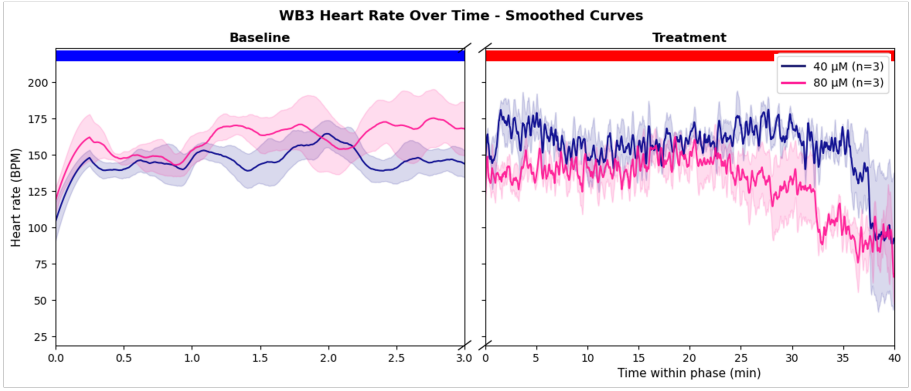

Figure 3.5: Heart rate responses across anesthetic conditions. (A) Ketamine. (B) Propofol. (C) WB3. Poorly tracked and noisy fish were excluded.

3.4 Whole-brain Light-sheet Imaging

Figure 3.6 and figure 3.7 show the population-wide calcium activity and the tail vigor before, during, and after the administration of 6 μM propofol for the fish that did and did not recover, respectively. The heatmap compares neuronal activity across the brain during treatment to baseline activity as measured by Ca^{2+} levels. The heatmap shows the values of $\Delta F/f$, which is the baseline normalized fluorescence. A value of zero means that the mean fluorescence level is at the baseline level, while a value of 1 means that the activity increased by 100% (2x activity), and a value of 2 means that the activity increased by 200% (3x activity). When propofol is perfused and administered, there is a reduction in activity characterized by the vertical bands of activity, as indicated by $\Delta F/f$ values decreasing. Once the propofol is washed out, the fish that recovers shows a gradual return of activity patterns, while activity remains suppressed for the fish that did not recover.

During baseline, prior to treatment with propofol, there are bursts of tail movement which stop after propofol is administered and the fish is anesthetized. In figure 3.6, the tail vigor recovery is associated with an increase in the calcium activity across the brain, showing recovery.

For the fish that did not recover, as seen in figure 3.7, there is a change in the band of activity at approximately 3950 seconds, where there is a decline in calcium levels. Right before this decline there is an increase in cellular activity, as shown by the red banding pat-

terns.

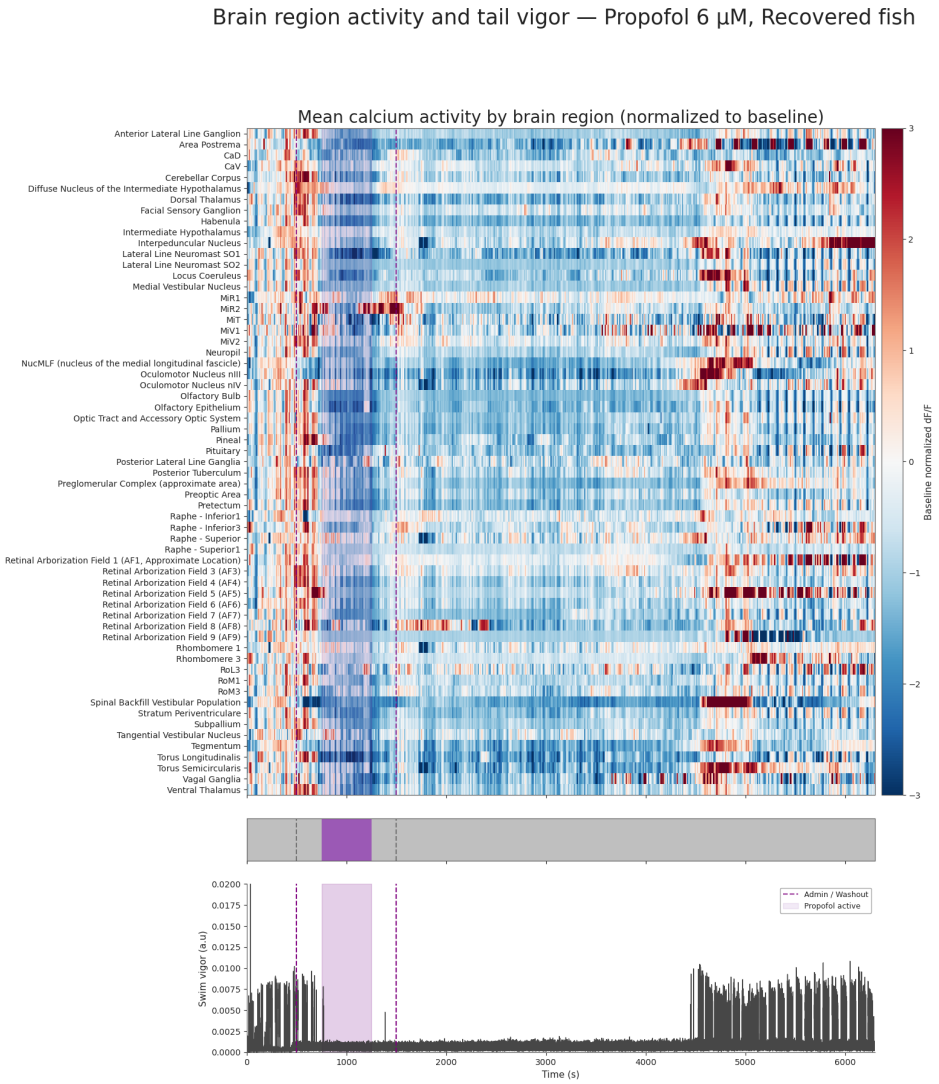

Figure 3.6: Calcium activity during 6 μM propofol treatment and washout in recovered fish. Light-sheet imaging experiments were performed by Marc Duque.

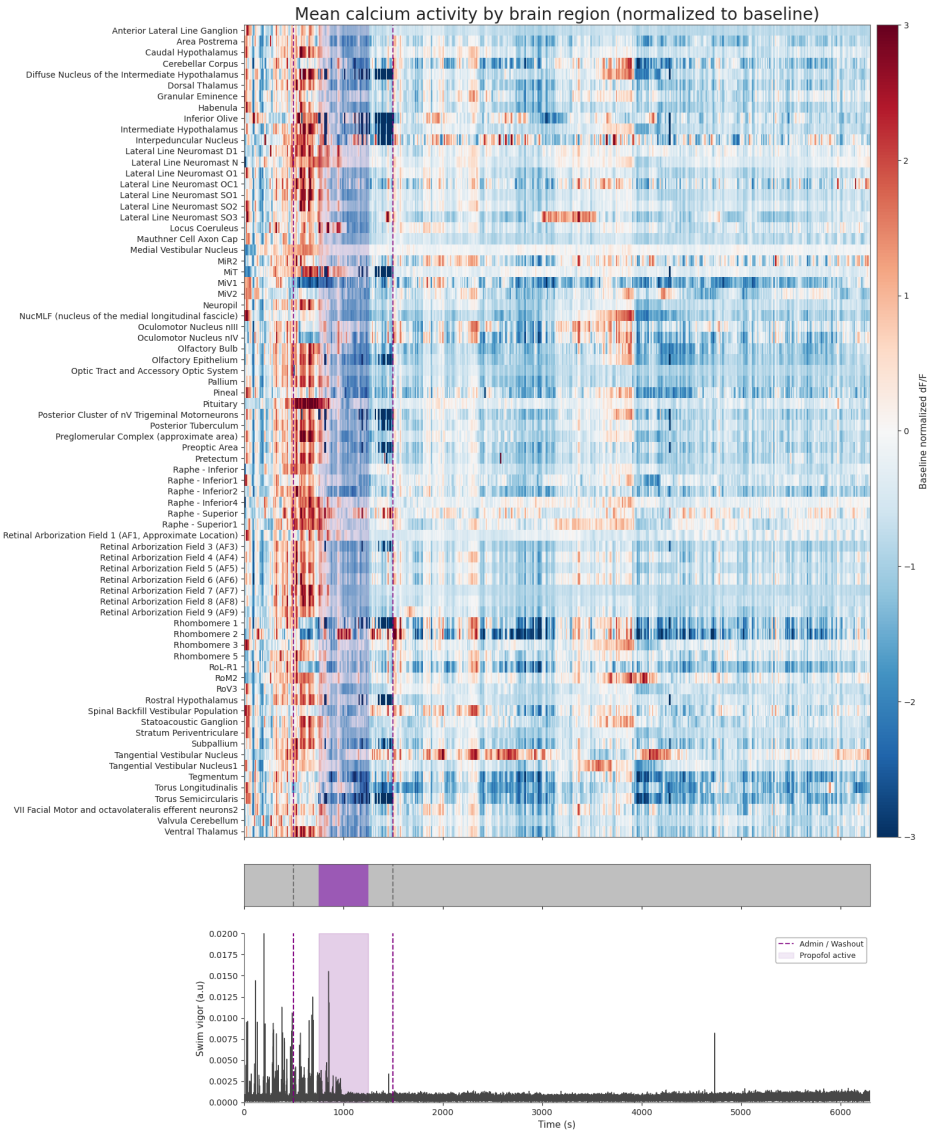

Figure 3.7: Calcium activity during 6 μM propofol treatment and washout in non-recovered fish. Light-sheet imaging experiments were performed by Marc Duque.

Figure 3.8 shows the mean fluorescence traces associated with the LC for the recovered and non-recovered fish. For both fish, there is a decline in LC activity during anesthesia, while the decline is much more pronounced for the fish that did not recover. LC activity is restored after physical recovery and peaks immediately as the fish starts swimming again.

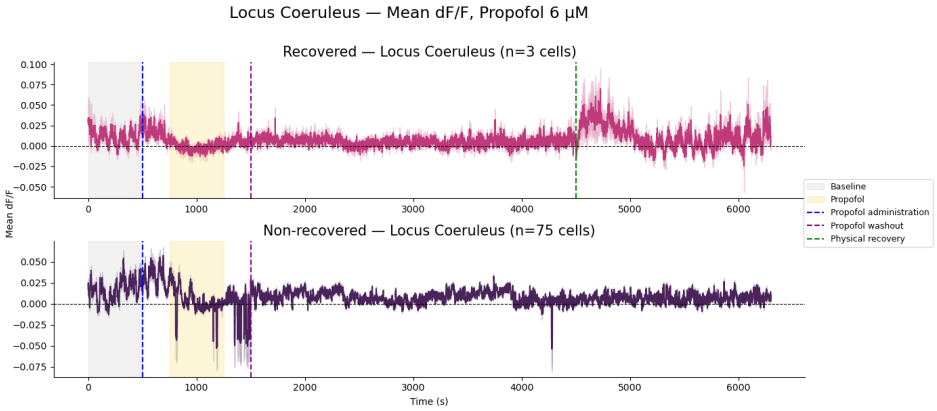

Figure 3.8: Locus coeruleus activity for recovered (top) and non-recovered (bottom) fish. Light-sheet imaging experiments were performed by Marc Duque.

Figure 3.9 shows the regions that had a significantly higher mean fluorescence during the physical recovery period (once the fish started swimming and tail vigor was restored) compared to baseline. A paired t-test was used to compare the activity of individual cells during baseline and after physical recovery. Figure 3.10 shows the traces of the mean fluorescence of these regions over time. The $\log_2$ FC values correspond to the log-base-2 fold change in fluorescence after emergence compared to baseline. A $\log_2$ FC value of 1 means that the region is 2x more active compared to baseline. The Retinal Arborization Field 5, interpeduncular nucleus, diffuse nucleus of the intermediate hypothalamus, raphe–superior, torus

semicircularis, and preglomerular complex showed the highest levels of significantly elevated activity. We only included regions with more than 20 cells registered. Not all regions are visibly discernible in the annotation due to differences in size and overlap.

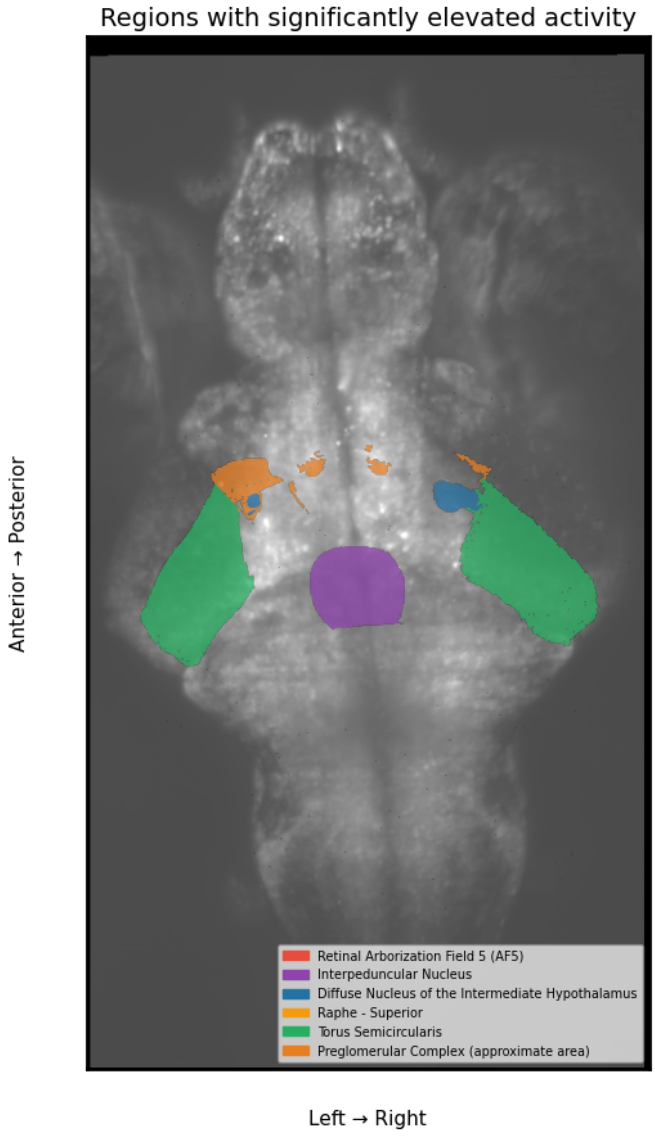

Figure 3.9: Anatomical annotation of regions with elevated activity after emergence for recovered fish. Light-sheet imaging experiments were performed by Marc Duque.

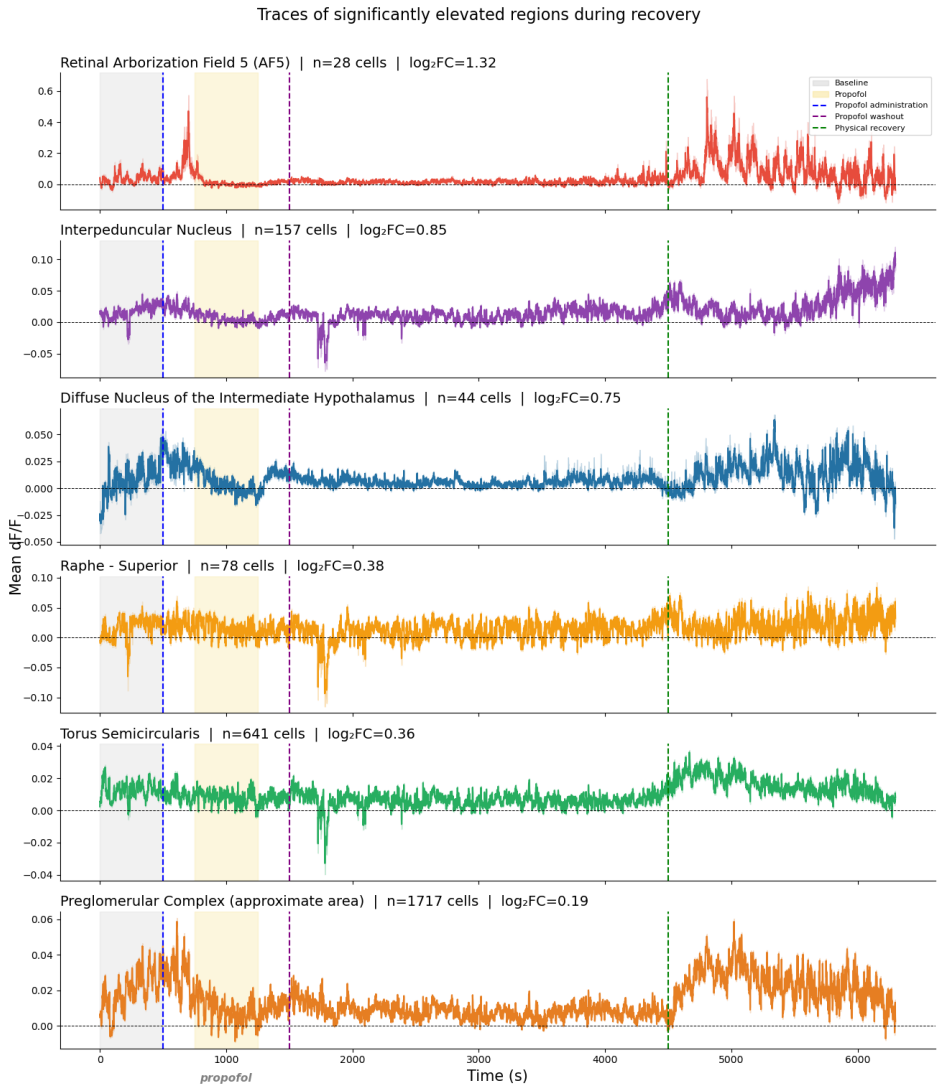

Figure 3.10: Traces of regions with elevated activity after emergence from 6μM propofol anesthesia compared to baseline for recovered fish. Light-sheet imaging experiments were performed by Marc Duque.

4

Discussion

Through the sets of experiments conducted as part of this thesis, we show the behavioral, physiological, and neural effects of commonly used and novel anesthetic compounds. This thesis presents the first analysis of the newly developed SNC80 derivative compound WB3 and investigates its potential as an anesthetic compound. We also present results on dose-dependent cardiac and behavioral responses to ketamine, propofol, and ketofol, a mixture

of both compounds.

4.1 Ketamine

As seen in panel A of figure 3.1, the effects of ketamine on swim bout rates, normalized to baseline, are consistent with the known rapid onset of ketamine-induced anesthesia. Recovery is also rapid; once the recovery recording is started promptly after washing the fish and transferring them to clean filtered fish water, some movement is observed.

Figure 3.2 shows that across all four tested ketamine concentrations, recovery turn angle distributions are moderately comparable to that of baseline, meaning that OMR response was restored to some degree. Compared to the averaged baseline turn angle distributions, ketamine-treated fish have higher density around 0º, showing overall reduced turn angle sensitivity and a higher propensity to swim forward even when presented with right or left-moving stimuli. Fish treated with 100 μg/mL ketamine display reduced bias toward the grating direction, swimming forward more and making fewer turns. This effect is comparatively higher than the optomotor distortion in fish treated with 50 μg/mL but lower than that of 150 μg/mL and 200 μg/mL treated fish, indicating that perhaps part of the observed effects could be explained by experimental conditions and imperfect tracking since no clear directionality can be established.

Our findings regarding the change in the ΔIID presented in figure 3.3 in spontaneously

free-swimming zebrafish without visual stimuli reveal that ketamine can result in decreased ΔIID in treated fish. For three of the four tested doses, the fish were closer to each other than predicted by random chance. Looking at the changes in the mean swimming speed for fish before and after treatment with anesthetics, there are no statistically significant changes except for fish treated with 200 μg/mL ketamine, which show an increase in speed during recovery. This indicates that speed remains largely stable from baseline to recovery once 80% of movement has been restored.

Zakhary et al. (2011) examined the effects of sub-anesthetic ketamine on zebrafish behavior. They found that treated zebrafish display rotational behavior, hyperactively swimming in circular patterns, while control zebrafish did not display any circling behavior. This circular motion could result in lower inter-individual distance, which would be consistent with our findings regarding patterns of ΔIID in recovery for ketamine-treated zebrafish.

Zakhary et al. (2011)'s findings have other implications for analyzing the observed ΔIID patterns as well. It is possible that altered locomotor activity is indirectly reducing spacing between fish. If ketamine causes circular patterns of swimming in fish, then it could be the case that the fish become spatially clustered without any specific increase in social affinity. This can also explain the trend that the average speed does not change from baseline to recovery while the ΔIID is reduced.

Overall, although the ΔIID is referenced as a measure of social spacing, it is capturing

the differences in the inter-fish distances from a null where neighbor trajectories are randomized. Thus, changes in motor activity could also explain the observed patterns without changes in social behavior. Further inquiry is required to determine the social consequences of ketamine exposure. It would be particularly useful to test older fish since they are known to be more social and display more shoaling behavior (Buske and Gerlai, 2011).

Ketamine did not result in significant cardiac suppression in any of the doses tested as part of this thesis. Guo et al. (2015) also found that ketamine results in a moderate decrease in the heart rate of treated *Xenopus* larvae. Our results show a slight downwards trend associated with ketamine administration, and the recovery heart rate is comparable to baseline, underscoring ketamine's strength as a compound in preserving cardiac function.

4.2 Propofol

The results of free-swimming behavior assays shown in panel B of figure 3.1 show that propofol causes very rapid locomotor sedation but slower recovery at both 15 and 30 μM. Compared to ketamine, propofol induced a deeper and more prompt state of anesthesia, and the bout rate returned gradually and not fully to baseline levels within the recording window. The lipophilic nature of propofol (Baker et al., 2005) can explain the lasting anesthesia due to accumulation in the fat tissue.

As seen in figure 3.2, propofol treated fish display dose-dependent OMR disruption

patterns. At the low propofol dose of 15 μM, the fish show nearly complete recovery of OMR, with turns in each direction being comparable to baseline. However, at 30 μM, the fish have less of a preference for the direction of the gratings and swim straight. This indicates that higher propofol doses can reduce directional responsiveness, which is consistent with previous observations regarding the longer recovery period associated with propofol-induced anesthesia.

As shown in panel B of figure 3.5, propofol displays the most notable dose-dependent cardiac suppression. At lower doses of 6, 10, and 15 μM, there is a downward trend associated with propofol administration. However, the decline is much more notable for 30 and 50 μM doses. It must be noted that there is a slight time delay from administering the anesthetic to restarting the recording, hence the discontinuous nature of the graphs and the heart rate having already decreased once the treatment recording is started. At 50 μM, the reduction in heart rate is most notable, and the cardiac activity does not recover by the end of the 100 minute recording period. The comparatively more gradual heart rate decline for fish treated with propofol 50 μM compared to lower concentrations could be explained by the speed of starting the treatment recording. The final treatment heart rate and the recovery heart rate are the lowest across all concentrations for the fish treated with 50 μM propofol. Across the different concentrations tested, the largest difference between the treatment and recovery heart rates is between the lowest dose at 6 μM and the intermediate doses at

10 and 15 μM. Fish treated with 6 μM propofol show preserved heart rate during treatment, whereas fish treated with 10 and 15 μM propofol displayed a larger decline in heart rate associated with treatment and slower incomplete recovery after washout. These results indicate that the cardiac effects of propofol are non-linear and can increase with small increases in dosage.

Propofol acts on the nervous system by activating aminobutyric acid receptors, resulting in CNS depression (Kotani et al., 2008), which can explain the sudden drop in cardiac activity. Moreover, propofol is known to cause bradycardia in human patients. The results presented in this thesis are consistent with findings in humans that propofol, especially at high doses, can result in extreme cardiovascular suppression. In humans, such bradycardia is more likely to occur with propofol compared to other anesthetic compounds (Tramèr et al., 1997), highlighting one of the clear limitations associated with this compound.

4.3 WB3

Our free-swimming stimulus-induced results in panel C of figure 3.1 show that in moderate concentrations, WB3 results in lagged anesthesia induction, but the recovery is also slow and movement does not return to the baseline levels at either tested dose of 80 and 100 μM. The novel anesthetic WB3 shows the slowest locomotor dynamics. Induction is comparatively delayed and recovery is also slow and incomplete.

Even though WB3 is shown to have lasting locomotor effects in terms of normalized to baseline bout rates, it brought about relatively small changes in OMR across both the 80 and 100 μg/mL doses. As seen in figure 3.2, the recovered turn angle distributions are less uniform than baseline. This shows that even though WB3-treated fish display OMR activity and directional sensitivity comparable to baseline, the recovered fish may exhibit subtle directional biases toward the direction of the moving gratings that were not initially present. This could indicate that although not all fish recover or recover to the baseline bout rate, the ones that do recover have preserved OMR.

The WB3 heart rate analyses performed as part of this experiment show that WB3, to our knowledge, is not a viable and appropriate anesthetic compound due to its extreme cardiovascular suppression which results in death in some cases. As seen in panel C of figure 3.5, there is a sudden and sharp drop by the end of the treatment period for both concentrations. Paired with the observed deaths, this indicates the possibility of acute toxicity or decompensation rather than gradual death caused by sedation. WB3 was shown to cause bradycardia in *Xenopus*, followed by weak and slow recovery. Sperry et al. (2024) speculate that this could be brought about by the lipophilic nature of WB3 that results in higher retention rates in the fat tissue.

As a novel analog of SNC80 that has a putative δ-opioid receptor pharmacophore removed, WB3 has an approximately 1000 times weaker δ-opioid binding compared to SNC80

(Sperry et al., 2024). Sperry et al. (2024) also report thermal proteome profiling for *Xenopus* tadpoles treated with SNC80 and identify non-opioid binding targets such as the Na^{2+}/Ca^{2+} exchanger 1, (NCX1). They note that NCX1 has been identified in cardiac tissue, hypothesizing that blocking Na^{2+}/Ca^{2+} activity could interrupt calcium influx into the mitochondria, slowing down ATP synthesis and thus interfering with cardiac activity. Ebert et al. (2005) found that disrupted calcium extrusion caused by a mutation in the NCX1h gene in the *tre* mutant zebrafish causes lethal cardiac arrhythmia in zebrafish embryos. They specifically report arrhythmia in the atrium with the tre ventricle being nearly silent, which could explain the sudden drop in the heart rate and cardiac collapse as observed in our results. Thus, if WB3's ion transport protein interactions are similar to those of SNC80, which could be reasonably assumed due to the non-opioid nature of these interactions and the fact that the only structural difference between WB3 and SNC80 is the removal of the δ-opioid pharmacore, then severe bradycardia, arrhythmia, and even abrupt cardiac failure are possible. Nevertheless, this hypothesis is formulated on the basis of the assumption of similar protein interactions and requires further investigation.

Therefore, although OMR is preserved after WB3 anesthesia, the high mortality and low recovery rates suggest that it is not, to our knowledge, an effective anesthetic.

4.4 Ketofol (Ketamine + Propofol)

In this thesis we present the first account, to our knowledge, of quantified behavioral and physiological responses to ketofol in zebrafish.

As seen in figure 3.3, fish treated with the low dose of ketofol display a statistically significant reduction in the ΔIID during recovery compared to baseline. Since fish treated with the higher dose of propofol do not show this trend, this observation may be driven by ketamine. However, there are several considerations to be taken into account. The tested dose of ketofol is low, and not all of the treated fish were anesthetized. Of the fish that were anesthetized, recovery was rapid due to the weakness of the administered solution, so the increase in activity, although calculated once movement is at 80% of baseline activity, could be explained by the fact that some fish were not anesthetized to begin with or experienced a relatively mild anesthesia that resulted in different recovery dynamics.

Our ketofol results in figure 3.5 show that the treatment heart rate is comparable to higher tested doses of ketamine and lower tested doses of propofol. During recovery, the ketofol heart rate was comparable to that of fish treated with higher doses of ketamine. This could be caused by the propofol. When comparing the tested dose of ketofol to propofol-treated fish, we see that the effects of ketofol (25 μg/mL ketamine and 3 μM propofol) were comparable to those of fish treated with 6 μM propofol. Thus, ketofol might bring about higher cardiac suppression than comparable single-dose treatments of ketamine.

Furthermore, the fact that ketamine and propofol have different degradation pathways support the potential use of both compounds in conjunction to ensure faster and more consistent recovery. Ketamine is mainly degraded through hepatic metabolism via the cytochrome P450 system. Ketamine is N-demethylated to norketamine, which still has anesthetic effects (Dinis-Oliveira, 2017). Propofol, on the other hand, in humans, is degraded by conjugation to propofol glucuronide and hydroxylation to 4-hydroxypropofol, both of which are water-soluble compounds (Dinis-Oliveira, 2018). The fact that these two pathways use different enzymes could in fewer residual compounds remaining, leading to faster recovery and decomposition of the anesthetic.

Our results indicate the potential of using ketofol to moderate the effects of each compound if used separately. By using the two compounds in conjunction, it may be possible to avoid the negative side effects of higher doses of ketamine and propofol. It is imperative to test higher doses of ketofol with different ketamine to propofol ratios to understand the interactions of the two compounds at different doses.

4.5 Comparison of Compounds

Our results are consistent with existing literature regarding the fast and short-acting effects of ketamine and the longer-lasting effects of propofol. We did not find WB3 to be as effective as the other two known compounds in bringing about anesthesia or regaining

baseline activity. We also find that anesthetic exposure overall affects zebrafish optomotor response during recovery. Under baseline conditions, the fish show a moderate directional bias toward the direction of the movement of the gratings. After recovery, this directionality is reduced, with the effects being more pronounced for propofol compared to others.

In relation to the observed trends regarding the decreased ΔIID, the stability in speed indicates that the results are not necessarily merely the byproduct of increased locomotion and faster swimming and could be indicative of changes to swim patterns or social affinity. The significant increase detected only at the 200 μg/mL dose of ketamine must be interpreted conservatively since this effect is not present in higher or lower tested doses.

The baseline heart rates across all experiments are consistent with existing literature that the embryonic heart rate for zebrafish is between 140-180 beats per minute, showing some degree of variability (Sarmah and Marrs, 2016). The observed differences in baseline heart rate can be attributed to variation in the batches of fish. We show that ketamine had the least significant cardiac suppression, followed by propofol, and WB3, which resulted in sudden cardiac collapse.

4.6 Whole-brain Imaging

Whole-brain calcium imaging of zebrafish treated with 6 μM propofol provides valuable insight into the brain-wide mechanism of action of anesthesia. We imaged one fish that did

and one that did not physically recover from after treatment with a low dose of propofol, allowing for a comparison between the two outcomes. As seen in figure 3.8, we found that mean fluorescence associated with locus coeruleus (LC) activity declined during propofol administration, which is consistent with the findings of Du et al. (2025), reporting a decrease in Ca^{2+} levels in presynaptic varicosities in the locus coeruleus norepinephrine (LC-NE) neurons. Due to imaging and alignment constraints, there are overall fewer cells registered to the atlas for the recovered fish compared to the non-recovered fish. Nonetheless, the suppression in LC fluorescence is much more pronounced for the fish that did not recover. This is consistent with the role of the LC in arousal. Given the fact that the LC is phylogenetically conserved across vertebrates (Hao et al., 2025), our results provide insight into potential anesthesia mechanisms of action and localized effects in humans.

Moreover, our results show that some regions have higher activity once the fish emerges from anesthesia compared to baseline. The Retinal Arborization Field 5 (AF5) showed the highest increase in activity after emergence, with mean fluorescence levels being 2.5x as high. This region is a visual center involved in optomotor reflexes. AF5 contributes to optokonetic and optomotor response (Orger et al., 2000) and whole-field motion (Dowell et al., 2025). This is consistent with the increase in AF5 activity once the fish starts swimming again in response to the visual stimulus. The interpeduncular nucleus (IPN) is located ventrally on the midline of the zebrafish brain, encoding directional turning rates (Dragomir

et al., 2020). The mean fluorescence increases over time as the fish regains locomotor activity, indicating OMR restoration. The diffuse nucleus of intermediate hypothalamus is a hypothalamic GAD1b cluster involved in sensorimotor modulation and response to visual stimuli (Heap et al., 2018), which is restored as locomotor function is regained. The dorsal raphe nucleus also showed increased activity. Yang et al. (2025) found that the dorsal raphe nucleus in zebrafish is suppressed by propofol. They report that the optogenetic activation of this region is associated with faster anesthesia recovery, while ablation of the DRN is associated with prolonged emergence in fish treated with 30 μM propofol. The torus semicircularis processes vibrational cues (Yáñez et al., 2024). The increase in activity in this region could be explained by the fish's response to water perception and self-generated movement as sensory feedback integration is restored upon anesthesia recovery. The preglomerular complex is the main source of visual and mechano-vibrational information relayed to the pallium (Trinh et al., 2025). It inputs sensory information to the dorsal telencephalon, which Yamamoto and Ito (2008) compared to the dorsal thalamus in mammals, which relays sensory information to the telencephalon. The regions that showed elevated activity during emergence from propofol highlight that there is an increase in activity in both sensory and arousal-associated nuclei when physical activity is restored. We hypothesize that the increase in activity compared to baseline can be explained by renewed sensory and motor feedback and a rebound of arousal systems.

Furthermore, we hypothesize that the sudden decrease in activity for the fish that did not recover at around 3950 seconds to be the point of neuronal cell death. Dekker et al. (2025) reported that the onset of neuronal death is followed by an increase in calcium levels, which can be observed before the drop in fluorescence levels throughout the brain at this time point.

4.7 Summary of Contributions

This thesis offers an investigation into the behavioral, physiological, and neural response of zebrafish larvae to known and newly developed anesthetic compounds. This work presents the first experiments on the effects of ketofol, a mixture of ketamine and propofol, on zebrafish cardiac and locomotor activity. Our experiments are also the first experiments to examine the anesthetic potency of the SNC80 derivative WB3 in zebrafish. The breadth of the anesthetic concentrations tested allow for a comprehensive comparative framework to understand anesthetic mechanism of action. Furthermore, free-swimming social experiments delineate the potential effects of these compounds even after locomotor activity has been restored, illustrating the need for further investigations to understand the longer-term effects of anesthetic compounds on behavior. Lastly, the light-sheet imaging data comparing whole-brain response are a step further toward understanding the specific brain regions involved in anesthesia induction and recovery.

4.8 Limitations

Although utmost care was devoted to the design and implementation of all experiments and analyses, our results are not without limitations. For all of the experiments discussed, the dosage that we could control was the nominal media concentrations and not the guaranteed tissue concentrations. Because zebrafish larvae have high skin permeability and can breathe as oxygen diffuses through their skin, we can administer the compound by exposing the larvae to a solution of the compound. However, internal tissue doses are largely affected by physicochemical properties and uptake. Therefore, the conclusions drawn from these results should primarily follow a comparative framework instead of a focus on the nominal concentrations.

Furthermore, as previously discussed, the discontinuous nature of the graphs highlight the time delay between stopping the recording for one phase of the experiment and starting the following phase after changing the treatment water. Thus, it is inevitable that the fish were exposed to and affected by the anesthetic or already recovered to some extent prior to starting the recording. This can explain the sharp declines in activity for the treatment phase of some concentrations and the existence of movement at the beginning of the recorded recovery phase.

Moreover, in our heart rate assays, the zebrafish were head-embedded in 2% agarose in filtered fish water solution. The head-embedded configuration of this experimental setup

can delay the diffusion of the anesthetic compared to the free swimming experiments where the animal models were directly and entirely exposed to the compound. Additionally, the tail data recorded as part of the head-embedded experiments lacked the required accuracy and spatial resolution to sufficiently quantify tail bouts and be used in analysis.

4.9 Future Directions

The results presented in this work show that WB3 is not a suitable anesthetic compound. However, the concrete molecular pathways of WB3 action on cardiac activity remain unknown. More specific cardiac analysis, as well as proteome profiling for WB3, could illustrate whether the hypothesized binding targets, such as NCX1, are affected by this compound.

Furthermore, all of the experiments conducted and presented in this thesis focus on larval zebrafish. Future research could explore other developmental stages to see whether the effects of these compounds remain consistent as the organism develops. Varying responses to the anesthetics could imply different mechanisms of action for anesthetic onset, anesthesia recovery, and social modulation.

Future extensions of this research could also focus on performing more light-sheet imaging studies to establish a comparative measure of whole-brain response to anesthesia. It would be particularly interesting to study the effects of ketofol on brain activity during and

after anesthesia to understand whether the whole-brain neural responses are significantly different than that of propofol and ketamine administered separately.

Bibliography

Ahrens MB, Orger MB, Robson DN, Li JM, Keller PJ (2013) Whole-brain functional imaging at cellular resolution using light-sheet microscopy. Nature Methods 10:413–420.

Ao Y, Yang B, Zhang C, Wu B, Zhang X, Xing D, Xu H (2021) Locus Coeruleus to Paraventricular Thalamus Projections Facilitate Emergence From Isoflurane Anesthesia in Mice. Frontiers in Pharmacology 12:643172.

Bademosi AT, Steeves J, Karunanithi S, Zalucki OH, Gormal RS, Liu S, Lauwers E, Verstreken P, Anggono V, Meunier FA, Van Swinderen B (2018) Trapping of Syntaxin1a in Presynaptic Nanoclusters by a Clinically Relevant General Anesthetic. Cell Reports 22:427–440.

Bahl A, Engert F (2020) Neural circuits for evidence accumulation and decision making in larval zebrafish. Nature Neuroscience 23:94–102.

Baker MT, Naguib M, Warltier DC (2005) Propofol: The Challenges of Formulation. Anesthesiology 103:860–876.

Brown EN, Pavone KJ, Naranjo M (2018) Multimodal General Anesthesia: Theory and Practice. Anesthesia & Analgesia 127:1246–1258.

Brown KE, Mirrakhimov AE, Yeddula K, Kwatra MM (2013) Propofol and the risk of delirium: Exploring the anticholinergic properties of propofol. Medical Hypotheses 81:536–539.

Buske C, Gerlai R (2011) Shoaling develops with age in Zebrafish (Danio rerio). Progress in Neuro-Psychopharmacology and Biological Psychiatry 35:1409–1415.

Cacciatore M, Magnani FG, Barbadoro F, Ippoliti C, Stanziano M, Clementi L, Nigri A, Nanetti L, Marino S, La Porta F, Lucca LF, Prada F, Leonardi M (2025) Thalamus and consciousness: a systematic review on thalamic nuclei associated with consciousness. Frontiers in Neurology 16:1509668.

Chitilian H, Eckenhoff R, Raines D (2013) Anesthetic drug development: Novel drugs and new approaches. Surgical Neurology International 4:2.

Dana H, Sun Y, Mohar B, Hulse BK, Kerlin AM, Hasseman JP, Tsegaye G, Tsang A, Wong A, Patel R, Macklin JJ, Chen Y, Konnerth A, Jayaraman V, Looger LL, Schreiter ER, Svoboda K, Kim DS (2019) High-performance calcium sensors for imaging activity in neuronal populations and microcompartments. Nature Methods 16:649–657.

Danielsson I, Gasior M, Stevenson G, Folk J, Rice K, Negus S (2006) Electroencephalographic and convulsant effects of the delta opioid agonist SNC80 in rhesus monkeys. Pharmacology Biochemistry and Behavior 85:428–434.

Davis MT, DellaGiogia N, Maruff P, Pietrzak RH, Esterlis I (2021) Acute cognitive effects of single-dose intravenous ketamine in major depressive and posttraumatic stress disorder. Translational Psychiatry 11:205.

De Velasco EMF, Law PY, Rodríguez RE (2009) Mu Opioid Receptor from the Zebrafish Exhibits Functional Characteristics as Those of Mammalian Mu Opioid Receptor. Zebrafish 6:259–268.

Dekker J, Lam W, Van Der Linde HC, Ophorst F, De Konink C, Schot R, Kremers G.-J, Sanderson LE, Berdowski WM, Van Woerden GM, Mancini GMS, Van Ham TJ (2025) The non-canonical thioreductase Tmx2b is essential for neuronal survival during zebrafish embryonic brain development. Development 152:dev204348.

Denomme N (2018) The Domino Effect: Ed Dominos early studies of Psychoactive Drugs. Journal of Psychoactive Drugs 50:298–305.

Dinis-Oliveira RJ (2017) Metabolism and metabolomics of ketamine: a toxicological approach. Forensic Sciences Research 2:2–10.

Dinis-Oliveira RJ (2018) Metabolic Profiles of Propofol and Fospropofol: Clinical and Forensic Interpretative Aspects. BioMed Research International 2018:1–16.

Dowell CK, Hawkins T, Bianco IH (2025) Subsets of extraocular motoneurons produce kinematically distinct saccades during hunting and exploration. Current Biology 35:554–573.e6.

Dragomir EI, tih V, Portugues R (2020) Evidence accumulation during a sensorimotor decision task revealed by whole-brain imaging. Nature Neuroscience 23:85–93.

Du W, Hu Y, Yang Y, Li J, Liu M, Zhang C, Wang Y, Xiang P, Yu Q, Du J, Wang Y (2025) Propofol inhibits norepinephrine release in vivo at presynaptic varicosities of locus coeruleus neurones in zebrafish larvae. British Journal of Anaesthesia 135:1704–1716.

Duque M, Chen AB, Hsu E, Narayan S, Rymbek A, Begum S, Saher G, Cohen AE, Olson DE, Li Y, Prober DA, Bergles DE, Fishman MC, Engert F, Ahrens MB (2025) Ketamine induces plasticity in a norepinephrine-astroglial circuit to promote behavioral perseverance. Neuron 113:426–443.e5.

Ebert AM, Hume GL, Warren KS, Cook NP, Burns CG, Mohideen MA, Siegal G, Yelon D, Fishman MC, Garrity DM (2005) Calcium extrusion is critical

for cardiac morphogenesis and rhythm in embryonic zebrafish hearts. Proceedings of the National Academy of Sciences 102:17705–17710.

Engeszer RE, Ryan MJ, Parichy DM (2004) Learned Social Preference in Zebrafish. Current Biology 14:881–884.

Forman SA, Miller KW (2016) Mapping General Anesthetic Sites in Heteromeric -Aminobutyric Acid Type A Receptors Reveals a Potential For Targeting Receptor Subtypes. Anesthesia & Analgesia 123:1263–1273.

García-Domínguez M (2025) -Opioid Receptor Agonists as Robust Pain-Modulating Agents: Mechanisms and Therapeutic Potential in Pain Modulation. Journal of Clinical Medicine 14:7263.

Guldenmund P, Vanhaudenhuyse A, Sanders R, Sleigh J, Bruno M, Demertzi A, Bahri M, Jaquet O, Sanfilippo J, Baquero K, Boly M, Brichant J, Laureys S, Bonhomme V (2017) Brain functional connectivity differentiates dexmedetomidine from propofol and natural sleep. British Journal of Anaesthesia 119:674–684.

Guo R, Liu G, Du M, Shi Y, Jiang P, Liu X, Liu L, Liu J, Xu Y (2015) Early ketamine exposure results in cardiac enlargement and heart dysfunction in Xenopus embryos. BMC Anesthesiology 16:23.

Hao M, Li F, Duan J.-W, Han M.-H (2025) Neural Circuit Connections and Functions of Locus CoeruleusNorepinephrine System. International Journal of Molecular Sciences 26:11163.

Hashimoto K (2019) Rapid-acting antidepressant ketamine, its metabolites and other candidates: A historical overview and future perspective. Psychiatry and Clinical Neurosciences 73:613–627.

Heap LA, Vanwalleghem GC, Thompson AW, Favre-Bulle I, Rubinsztein-Dunlop H, Scott EK (2018) Hypothalamic Projections to the Optic Tectum in Larval Zebrafish. Frontiers in Neuroanatomy 11:135.

Heras FJH, Romero-Ferrero F, Hinz RC, De Polavieja GG (2019) Deep attention networks reveal the rules of collective motion in zebrafish. PLOS Computational Biology 15:e1007354. Ed. by Battaglia FP.

Höflich A, Kraus C, Pfeiffer RM, Seiger R, Rujescu D, Zarate CA, Kasper S, Winkler D, Lanzenberger R (2021) Translating the immediate effects of S-Ketamine using hippocampal subfield analysis in healthy subjects-results of a randomized controlled trial. Translational Psychiatry 11:200.

Howe K et al. (2013) The zebrafish reference genome sequence and its relationship to the human genome. Nature 496:498–503.

Jutkiewicz EM, Kaminsky ST, Rice KC, Traynor JR, Woods JH (2005) Differential Behavioral Tolerance to the -Opioid Agonist SNC80 ([(+)-4-[(R)--[(2 S,5 R)-2,5-Dimethyl-4-(2-propenyl)-1-piperazinyl]-(3-methoxyphenyl)methyl]-N,N-diethylbenzamide) in Sprague-Dawley Rats. The Journal of Pharmacology and Experimental Therapeutics 315:414–422.

Kämmer N, Reimann T, Braunbeck T (2024) Neurotoxic pesticides change respiratory parameters in early gill-breathing, but not in skin-breathing life-stages of zebrafish (Danio rerio). Aquatic Toxicology 267:106831.

Kohtala S (2021) Ketamine50 years in use: From anesthesia to rapid antidepressant effects and neurobiological mechanisms. Pharmacological Reports 73:323–345.

Kongsayreepong S, Cook DJ, Housmans PR (1993) Mechanism of the Direct, Negative Inotropic Effect of Ketamine in Isolated Ferret and Frog Ventricular Myocardium. Anesthesiology 79:313–322.

Kotani Y, Shimazawa M, Yoshimura S, Iwama T, Hara H (2008) The Experimental and Clinical Pharmacology of Propofol, an Anesthetic Agent with Neuroprotective Properties. CNS Neuroscience & Therapeutics 14:95–106.

Lister JA, Robertson CP, Lepage T, Johnson SL, Raible DW (1999) Nacre encodes a zebrafish microphthalmia-related protein that regulates neural-crest-derived pigment cell fate. Development (Cambridge, England) 126:3757–3767.

Lundström S, Zachrisson U, Fürst CJ (2005) When Nothing Helps: Propofol as Sedative and Antiemetic in Palliative Cancer Care. Journal of Pain and Symptom Management 30:570–577.

Lynch DK (2015) Snells window in wavy water. Applied Optics 54:B8.

Metcalf MD, Yekkirala AS, Powers MD, Kitto KF, Fairbanks CA, Wilcox GL, Portoghese PS (2012) The Opioid Receptor Agonist SNC80 Selectively Activates Heteromeric Opioid Receptors. ACS Chemical Neuroscience 3:505–509.

Mion G, Villevieille T (2013) Ketamine Pharmacology: An Update (Pharmacodynamics and Molecular Aspects, Recent Findings). CNS Neuroscience & Therapeutics 19:370–380.

Mwaffo V, Zhang P, Romero Cruz S, Porfiri M (2017) Zebrafish swimming in the flow: a particle image velocimetry study. PeerJ 5:e4041.

ONeale A, Ellis J, Creton R, Colwill RM (2014) Single stimulus learning in zebrafish larvae. Neurobiology of Learning and Memory 108:145–154.

Orger MB, Smear MC, Anstis SM, Baier H (2000) Perception of Fourier and non-Fourier motion by larval zebrafish. Nature Neuroscience 3:1128–1133.

Palmér T, Ek F, Enqvist O, Olsson R, Åström K, Petersson P (2017) Action sequencing in the spontaneous swimming behavior of zebrafish larvae - implications for drug development. Scientific Reports 7:3191.

Purdon PL, Pierce ET, Mukamel EA, Prerau MJ, Walsh JL, Wong KFK, Salazar-Gomez AF, Harrell PG, Sampson AL, Cimenser A, Ching S, Kopell NJ, Tavares-Stoeckel C, Habeeb K, Merhar R, Brown EN (2013) Electroencephalogram signatures of loss and recovery of consciousness from propofol. Proceedings of the National Academy of Sciences 110.

Reed SJ, Plourde G (2015) Attenuation of High-Frequency (50-200 Hz) Thalamocortical EEG Rhythms by Propofol in Rats Is More Pronounced for the Thalamus than for the Cortex. PLOS ONE 10:e0123287. Ed. by Ward LM.

Renier C, Faraco JH, Bourgin P, Motley T, Bonaventure P, Rosa F, Mignot E (2007) Genomic and functional conservation of sedative-hypnotic targets in the zebrafish. Pharmacogenetics and Genomics 17:237–253.

Robinson DH, Toledo AH (2012) Historical Development of Modern Anesthesia. Journal of Investigative Surgery 25:141–149.

Sahinovic MM, Struys MMRF, Absalom AR (2018) Clinical Pharmacokinetics and Pharmacodynamics of Propofol. Clinical Pharmacokinetics 57:1539–1558.

Sara SJ, Bouret S (2012) Orienting and Reorienting: The Locus Coeruleus Mediates Cognition through Arousal. Neuron 76:130–141.

Sarmah S, Marrs J (2016) Zebrafish as a Vertebrate Model System to Evaluate Effects of Environmental Toxicants on Cardiac Development and Function. International Journal of Molecular Sciences 17:2123.

Schnoebel R, Wolff M, Peters SC, Bräu ME, Scholz A, Hempelmann G, Olschewski H, Olschewski A (2005) Ketamine impairs excitability in superficial dorsal horn neurones by blocking sodium and voltage-gated potassium currents. British Journal of Pharmacology 146:826–833.

Seamans J (2008) Losing inhibition with ketamine. Nature Chemical Biology 4:91–93.

Shin TJ, Kim P.-J, Choi B (2022) How general anesthetics work: From the perspective of reorganized connections within the brain. Korean Journal of Anesthesiology 75:124–138.

Son Y (2010) Molecular mechanisms of general anesthesia. Korean Journal of Anesthesiology 59:3.

Sperry MM, Charrez B, Fotowat H, Gardner E, Pilobello K, Izadifar Z, Lin T, Kuelker A, Kaki S, Lewandowski M, Lightbown S, Martinez R, Marquez S, Moore J, Plaza-Oliver M, Sesay AM, Shcherbina K, Sheehan K, Takeda T, Del Campo D, Andrijauskaite K, Cisneros E, Lopez R, Cano I, Maxwell Z, Jessop I, Veraza R, Bunegin L, Percival TJ, Yracheta J, Pena JJ, Wood DM, Homas ZT, Hinshaw CJ, Cox-Hinshaw J, Parry OG, Sleeter JJ, Weitzel EK, Levin M, Super M, Novak R, Ingber DE (2024) Identification of pharmacological inducers of a reversible hypometabolic state for whole organ preservation. eLife 13:RP93796.

Tanaka R, Zhou B, Agrochao M, Badwan BA, Au B, Matos NC, Clark DA (2023) Neural mechanisms to incorporate visual counterevidence in self-movement estimation. Current Biology 33:4960–4979.e7.

Tramèr MR, Moore RA, McQuay HJ (1997) Propofol and bradycardia: causation, frequency and severity. British Journal of Anaesthesia 78:642–651.

Trinh A.-T, Ostenrath AM, Del Castillo-Berges I, Kraus S, Cachin F, Serneels B, Kawakami K, Yaksi E (2025) Hierarchical processing of sensory information across topographically organized thalamocortical-like circuits in the zebrafish brain.

Yamamoto N, Ito H (2008) Visual, lateral line, and auditory ascending pathways to the dorsal telencephalic area through the rostrolateral region of the lateral preglomerular nucleus in cyprinids. Journal of Comparative Neurology 508:615–647.

Yáñez J, Eguiguren MH, Anadón R (2024) Neural connections of the torus semicircularis in the adult Zebrafish. Journal of Comparative Neurology 532:e25586.

Yang X, Zhu S, Xia M, Sun L, Li S, Xiang P, Li F, Deng Q, Chen L, Zhang W, Wang Y, Li Q, Lyu Z, Du X, Du J, Yang Q, Luo Y (2025) The Serotonergic Dorsal Raphe Promotes Emergence from Propofol Anesthesia in Zebrafish. The Journal of Neuroscience 45:e2125232025.

Zakhary SM, Ayubcha D, Ansari F, Kamran K, Karim M, Leheste JR, Horowitz JM, Torres G (2011) A behavioral and molecular analysis of ketamine in zebrafish. Synapse 65:160–167.

Zaki HA, Shalik N, Shaban E, Bashir K, Iftikhar H, Mohamed Khair Y, Abdelrahim MG, Fayed M, Hendy M, Salem EE.-D, Elmoheen A (2022) An Analytical Comparison Between Ketamine Alone and a Combination of Ketamine and Propofol (Ketofol) for Procedural Sedation and Analgesia From an Emergency Perspective: A Systematic Review and Meta-Analysis. Cureus.